SEA GRANT

DISSERTATION SERIES

Institute for Marine and Coastal Studies
University of Southern California
Los Angeles, California 90007

The **Institute for Marine and Coastal Studies** was founded by the University of Southern California in 1975 to be the institutional framework for its marine programs, many of which had been in operation since the early 1900s. The Institute promotes basic and applied research as well as training in marine studies; sponsors workshops, conferences, and extension courses; and produces reports and publications based on Institute-sponsored research. The work of the Institute takes place throughout the southern California region—at USC's University Park campus, on several research vessels, at research facilities located at the Port of Los Angeles, and at the Catalina Marine Science Center on Santa Catalina Island.

For additional copies of this paper, or for more information about the Institute for Marine and Coastal Studies, write to:

The Institute for Marine and Coastal Studies
University of Southern California
Los Angeles, California 90007
Telephone: (213) 741-6840

THE EFFECTS OF BIOLOGICAL ACTIVITY ON TRANSPORT OF DISSOLVED SPECIES ACROSS THE SEDIMENT-WATER INTERFACE OF SAN FRANCISCO BAY

by

Michael Anthony Korosec

USCSG-TD-04-79 November 1979

This work is the result of research sponsored by the NOAA Office of Sea Grant, Department of Commerce, under grant no. USC NOAA 04-8-M01-186. The U.S. government is authorized to produce and distribute reprints for governmental purposes, notwithstanding any copyright notation that may appear hereon.

Institute for Marine and Coastal Studies
University of Southern California
University Park
Los Angeles, California 90007
November 1979

THE EFFECTS OF BIOLOGICAL ACTIVITY ON TRANSPORT OF DISSOLVED SPECIES ACROSS THE SEDIMENT-WATER INTERFACE OF SAN FRANCISCO BAY

by

Michael Anthony Korosec

A Thesis Presented to the
FACULTY OF THE GRADUATE SCHOOL
UNIVERSITY OF SOUTHERN CALIFORNIA
In Partial Fulfillment of the
Requirements for the Degree
MASTER OF SCIENCE
(Geological Sciences)

January, 1979

ACKNOWLEDGEMENTS

This project was made possible by funding under Grant No. OCE 76-81154 from the National Science Foundation and Grant No. 04-7-158-44113 from the National Oceanographic and Atmospheric Administration, Office of Sea Grant, Department of Commerce.

I would like to thank John Conomos and Dave Peterson, along with other members of their Estuarine Studies Team at the U.S. Geological Survey, Menlo Park, California, for their provision of ship time, equipment, and advice on San Francisco Bay and some of the finer restaurants in the area.

Fellow students Larry Miller, Chris Fuller, and Blayne Hartman offered their time and expertise in the field and laboratory. I thank them for solving problems and keeping me honest.

My appreciation is extended to Dr. Teh-Lung Ku and Dr. Ronald Kolpack for their comments and critiques, leading to the final report.

Typist Pam Whitlock and draftsman Gibb Johnson of the State of Washington Division of Geology and Earth Resources provided their professional skills and talents, and deserve credit for all esthetic considerations.

Special thanks go to Dr. Douglas Hammond, whose continuous guidance through frustrating Socratic methods pro-

duced a phoenix from what may have otherwise been ashes, and to all the friends and lovers who put up with me through the ordeal.

TABLE OF CONTENTS

LIST OF FIGURES

LIST OF FIGURES (Cont.)

LIST OF TABLES

ABSTRACT

Concentration vs. depth profiles for dissolved T-CO_2, NH_4^+, PO_4^{-3}, SiO_2, and Rn measured in San Francisco Bay sediment pore water suggest that biologically induced transport produces nutrient fluxes greater than those produced by molecular diffusion alone. On the basis of observed profiles, three models have been proposed to quantify this transport.

Model 1 treats burrowing activities of macro-organisms as a diffusive transport process. The sediments are considered as a two-box system, with a stirred aerobic upper zone and an undisturbed anaerobic zone below. An effective diffusivity constant is determined for T-CO_2 with the model and applied to the concentration gradients to calculate nutrient fluxes. Fluxes of T-CO_2, NH_4^+, PO_4^{-3}, and SiO_2 from the upper box to the water column are found to be an order of magnitude greater than fluxes from the lower box to the sediments above.

Model 2 treats irrigation of sediments by polychaetes as an advective process. Again, a two-box system is considered as this irrigation produces aerobic conditions in the upper zone of the sediments. The areal pumping rate of the polychaetes is determined by constructing a radon-222 mass balance and is used with sediment pore water and water

column concentrations to determine the net flux from the sediments.

Model 3 treats burrowing activity as a means by which surface area exposed to estuarine waters is increased. The observed burrow surface area from core radiographs showed there to be about 10 cm^2 of surface per cm^2 of bottom. This produces 10 times the surface area over which molecular diffusion can occur.

Fluxes calculated by the three models are of the same order of magnitude and comparable to rates observed in benthic chamber experiments. The average fluxes calculated with the three models for T-CO_2, NH_4^+, and SiO_2 are 10 $\pm$ 6.7, 2.3 $\pm$ 3, and 5 $\pm$ 3.6 mMol/m^2/day, respectively.

Rates calculated from the models are used along with previously published data to construct a rough budget for San Francisco Bay. The rate of nutrient regeneration in the sediments is about 1/2 that of the water column. The resulting carbon flux from the sediments is about 1/6 the value of gross carbon assimilation rates for primary productivity, and 1/4 the net rate.

Comparison of pore water extraction techniques shows centrifugation and squeezing of sediments to produce similar results, which are further supported by peeper sampling results. Large discrepancies are sometimes noted, but can be attributed to spatial variation within the sediments.

INTRODUCTION

The growth and maintenance of estuarine life are primarily controlled by the availability of primary nutrients to the phytoplankton. Nitrogen, phosphorous, carbon, and silica initially enter an estuarine system through rivers where they may be taken up by phytoplankton. As individuals live, grow, reproduce, and die, nutrients are continuously cycled through the water column and interstitial waters of the sediments. Eventually, these nutrients will be lost to the ocean and the atmosphere, or buried within the sediments.

In determining a nutrient budget for a system, the difficulty lies in assessing the extent and significance of the various sites of nutrient regeneration. By examining nutrient regeneration and mass transport processes in the sediments of the San Francisco Bay estuarine system, this study will demonstrate the significance of interface exchange and the relative importance of the physical, chemical, and biological controls on this process.

Metabolism of organic material in sediments usually results in a buildup of dissolved nutrients in the interstitial waters. The concentration in the near shore marine and estuarine sediments may reach levels two orders of magnitude greater than the concentrations in the water column

(Berner, 1964, and Sholkovitz, 1973). Several detailed kinetic models for organic material diagenesis have been developed by Berner (1974, 1975, and 1977) for anoxic marine sediments. These models assume that vertical concentration gradients in pore waters are greater than lateral gradients, and therefore treat early diagenesis in terms of one dimension (Berner, 1971). Fluxes due to molecular diffusion for a dissolved species c are calculated from Fick's First Law:

$$\text{Flux} = J_{MD} = D_s \, (dc/dx) \qquad \text{Eq. 1}$$

where D_s is the coefficient of molecular diffusion and dc/dx is the vertical concentration gradient. By introducing terms for sedimentation rate and reactions, a steady state diagenetic relationship can be developed for each nutrient species (Berner, 1975 and 1977). Most sediments are not deposited under steady state conditions, but the use of such an idealized case makes possible the development of simple equations which facilitate the assessment of chemical species' relationships.

For anoxic sedimentary environments, such as some offshore basins and deep lake bottoms, molecular diffusion is the dominant transport process. For bottom sediments exposed to oxygenated waters, however, bacterial activity and transport mechanisms may be greatly effected by the

different chemical environment and perturbation created by the benthic fauna. San Francisco Bay provides a test area for an examination of the effects of biological activity on nutrient transport through estuarine sediments.

San Francisco Bay

San Francisco Bay (Figure 1) is a complex estuarine system, with open bays, deep narrow channels, tidal marshes, mud flats, and sloughs. The most extensive environment is the shallow water bays, only a few meters deep at low tide. Several geostatistics are listed in Table 1.

On the basis of water circulation, San Francisco Bay can be divided into two systems. The northern portion of the Bay receives fresh water primarily from the San Joaquin-Sacramento River system and oceanic waters through the Golden Gate. These waters are mixed by the tides and flushed out of the system by density-driven circulation which depends on river discharge (McCulloch et al, 1970).

The South Bay does not have a major fresh water discharge at its head, only a few creeks and waste water outfalls around its perimeter. Flushing depends primarily on tidal mixing with Central Bay waters, although river discharge at the San Joaquin-Sacramento River delta has been reported to have an effect on South Bay flushing (McCulloch

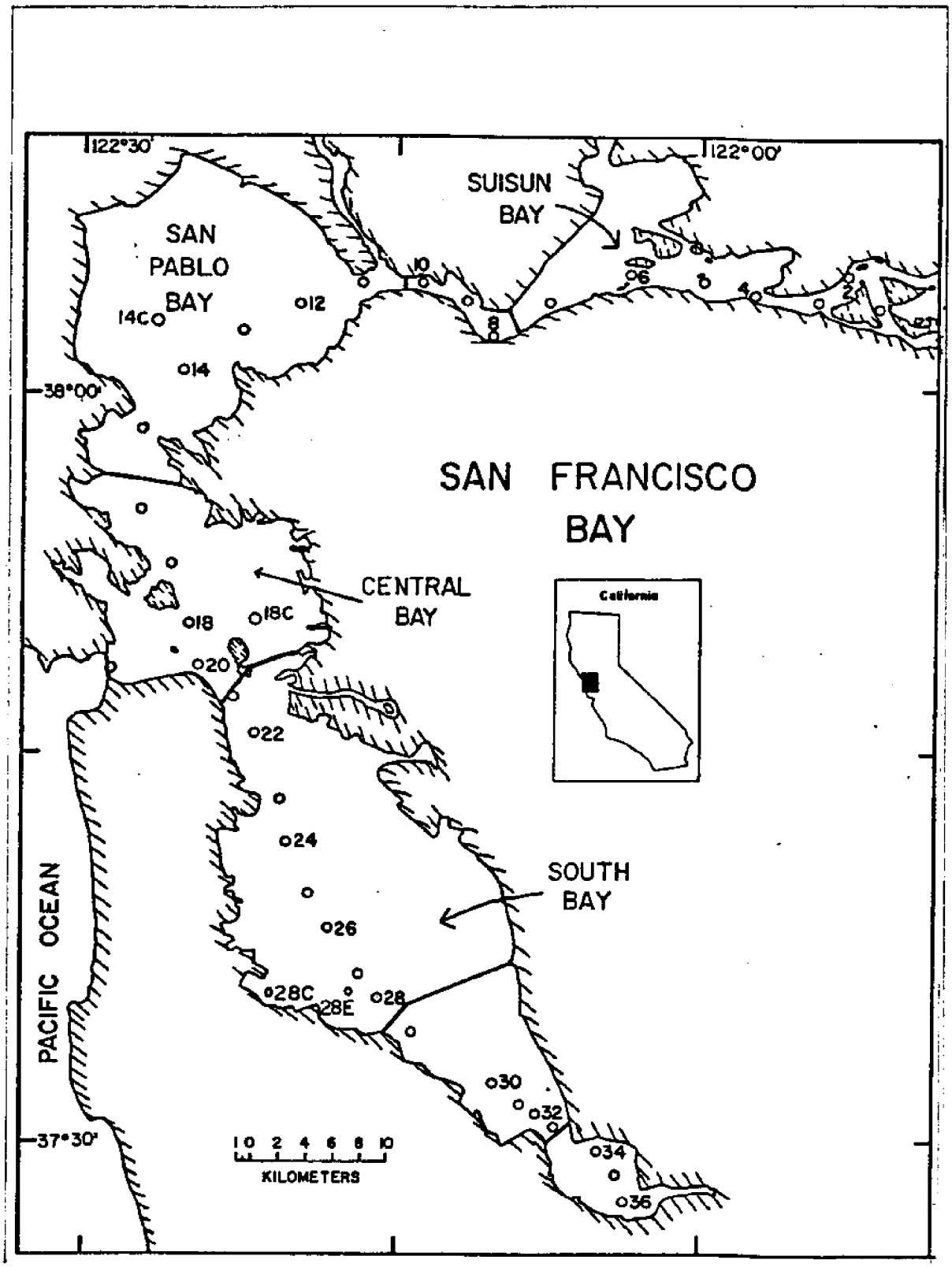

Figure 1. San Francisco Bay Station Locations.

TABLE 1

San Francisco Bay Geostatistics

Area (at MLLW) Including mudflats	1.04×10^9 m^2 1.24×10^9 m^2
Volume	6.66×10^9 m^3
Average Depth	6.1 m
River Discharge (Annual)	20.9×10^9 m^3
Suspended sediment inflow (Annual)	4.2×10^6 metric tons
Sediment Accumulation Rate	350 $mg/cm^2/yr$ 1 $mg/cm^2/day$ 2 mm/yr

After Conomos and Peterson (1977)

et al, 1970). The result is longer residence times for the water and dissolved species in South Bay than in other parts of the system.

Waters flowing to the Bay from the San Joaquin-Sacramento drainage basin carry a significant sediment load, most of which passes through the delta and into the Bay (Pestrong, 1970). This is supplemented by sediment carried into the Bay system by smaller streams draining the surrounding hills and by direct runoff. The rates of input vary greatly during the year, along with the river discharge and seasonal rainfall (Conomos and Peterson, 1977). The annual sediment load, integrated over the entire Bay, results in an average sediment accumulation of 350 mg/cm^2/year, or 2 mm/yr of silty clay.

The distribution and abundance of benthic organisms living in San Francisco Bay have been the subjects of numerous studies over the last half century (Nichols, 1973). A diverse marine fauna extends from the Golden Gate through the Central and South Bays. The genera and most of the species are similar to those found on the continental shelf off central California. At the northeastern end of the Bay, near the delta, a fresh water-brackish fauna exists, comparatively low in number and diversity. The transition zone between these extreme environments is inhabited by a stenohaline fauna, where genera are common to

most estuaries (Nichols, 1973). Filice (1958) provides a description of the various benthic invertebrates found in the Bay.

Previous Nutrient Studies

Water column nutrient budgets have been constructed for several estuarine systems, including the Potomac (Jaworski et al, 1972), the Pamlico River Estuary of North Carolina (Hobbie et al, 1975), Chesapeake Bay (McCarthy et al, 1975), and the Hudson River (Simpson et al, 1975). Dissolved silica in San Francisco Bay waters has been studied by Storrs et al (1963 and 1964), Bain and McCarty (1965), and Peterson et al (1975). Bain and McCarty (1965) and Peterson (1978) also examined species of nitrogen and phosphorous in this system and related these nutrients to productivity studies.

The chemistry of nutrients in interstitial waters has been studied recently in nearshore marine sediments (Jorgensen, 1977a and 1977b, Vanderborght et al, 1977a and 1977b, and Whelan, 1974), in offshore basins (Rittenberg et al, 1955, and Sholkovitz, 1973), and in fresh water lakes (Hesslein, 1976a). Studies of estuarine interstitial water nutrients are relatively fewer in number, most notable of which include the Narragansett Bay (Hale, 1974,

Nixon et al, 1976, and McCaffrey et al, 1978), Puget Sound (Grundmanis and Murray, 1977), and the Chesapeake Bay (Matisoff et al, 1975).

The importance of sedimentary nutrient regeneration for the construction of nutrient budgets varies from system to system. In the Hudson River Estuary, phosphate flux from the sediments was shown to be a minor contributor to the total budget (Simpson et al, 1975), with input from sewage outfalls and rivers providing 80 to 90 percent of the daily nutrient flux to the water column. For Chesapeake Bay, diffusive flux across the sediment-water interface was calculated to provide no more than 5 percent of the total water column phosphate per week (Bray et al, 1973). On this basis, McCarthy et al (1975) neglect flux from the sediments in their nutrient budget for Chesapeake Bay.

According to Hale (1974) and Nixon et al (1976), the flux resulting from nutrient regeneration in the sediments represents 80 percent of the nitrogen and phosphorous entering the water column of Narragansett Bay. This value changes with the seasons since the release of nutrients from the sediments is regulated by rates at which organic detritus reaches the sediments, rates at which the detritus is decomposed by aerobic and anaerobic bacteria, and rates

at which the nutrients are transported through the sediments (McCaffrey et al, 1978).

PROCEDURES AND TECHNIQUES

Sample Collection

Figure 1 shows the San Francisco Bay study area and the station numbers which refer to the USGS location system. Descriptions of these stations are given in Appendix A.

In the months of March, July, and October of 1977, the USGS Research Vessel POLARIS was used to sample the northern bays and the mid-channel areas of South Bay, while a whaler provided access to the more shallow areas of the Bay. Sediment cores were collected with a modified Phleger corer using a 5 cm I.D. plastic liner. A few cores were taken by divers in the shallow flats. Most cores were about 35 to 40 cm in length, with a few as long as 70 cm.

In addition, several cores were collected from the San Pedro Harbor of Los Angeles in February 1978 for testing techniques. These cores were taken with the modified Phleger corer from a whaler.

Pore Water Extraction

Within 5 hours after the cores had been collected, the sediments were extruded in 3 or 4 cm intervals. Water was

extracted immediately from these intervals by centrifugation at 2570 x g for 3 to 6 minutes, removed from centrifuge tubes by syringe, and passed through a 0.4 μm Nuclepore filter held in a plastic Swinex holder.

On several cores, a second method of extraction was used. This method employs a modified Reeburgh squeezer (Reeburgh, 1967) with helium gas to push pore water through a Whatman # 40 and 0.4 um Nuclepore filter. Blank runs in which deionized water was passed through these filters showed no appreciable contamination for ammonia, phosphate, and silicate. The volume of pore water extracted by the squeezing method was typically less than 5 to 8 ml; whereas, 10 to 15 ml could be obtained from similar sediment in a shorter time using centrifugation. For these reasons, centrifugation was the preferred method.

Extracted pore waters were collected in precleaned polyethylene vials. One ml was removed with a syringe for immediate analysis for Total CO_2.

During the July and October 1977 cruises to San Francisco Bay, and the February 1978 San Pedro Harbor cruise, two other techniques, pore water peepers and benthic chambers, were used to assess the flux of species from the sediments to the water column. The primary work was carried out by other members of the lab: Miller, Hammond, and Fuller.

Pore Water Peepers

To avoid the problems involved in coring sediments, such as compaction, interface disruption, and degassing, Hesslein (1976) developed a "pore water peeper". The procedure involves the equilibration of pore water with deionized water in small chambers at discrete depths through a dialysis membrane. The small chambers are cut into a solid plexiglass rod (3 cm O.D.) at 1 cm intervals. Hesslein (1976) gives a detailed technical description of this device.

Repeated time sequence experiments showed great variation in the time needed for equilibration for the different species. By leaving the peepers in for 8 days, waters were at least 85 percent equilibrated for chloride, with the top intervals reaching 100 percent equilibrium. This is further discussed in Appendix D.

Benthic Chambers

To determine the absolute value of the flux of species from the sediment pore waters, benthic chambers were used. Plexiglass boxes (20 cm x 20 cm x 10 cm high) were placed on the sediment surface by divers and sampled over 1 to 2 day periods. Changes in concentration of species in the water above the sediments in these closed, mechanically

mixed chambers were determined over time intervals of 3 to 24 hours. The design and sampling procedures were based on schematics of benthic flux chambers and techniques described by Hesslein (1976).

Chemical Determinations of Species Concentrations

The techniques used to determine species concentrations are listed in Table 2. The estimated precision of each method was determined by running replicate standards and samples. The precisions for ammonia, phosphate, and silicate agree with those reported by Strickland and Parsons (1972).

The T-CO_2, total concentration of all species of dissolved oxidized inorganic carbon, was determined by the method described by Hammond (1975). A 1 ml sample was injected into a glass stripping chamber containing about 0.2 ml of 5 N sulfuric acid. The chamber was continuously purged with helium through a $CaSO_4$ pre-column (10 cm x 6 mm I.D.) at 40 cc/min into a Carle 311 Gas Chromatograph equipped with a silica gel column (150 cm x 5 mm O.D.) at 40° C. Detector sensitivity was determined by injecting a known volume of a standard CO_2 gas. Ammonia was determined colorimetrically by the method of Solorozano (1969), as modified for pore waters by Presley

Table 2

Analytical Techniques

Species	Technique	Precision	Reference
$T\text{-}CO_2$	Gas Chromatography	± 3%	Hammond (1975)
NH_4^+	Colorimetric	± 10%	Solorozano (1969) Presley (1971)
PO_4^{-3}	Colorimetric	± 4%	Murphy & Riley (1962)
SiO_2	Colorimetric	± 5%	Mullin & Riley (1955)
$SO_4^=$	$^{133}BaSO_4$ precipitation with Gamma Counting	± 10%	--
Cl^-	Titration	± 1%	--

Note: Precision is based on duplicate analyses of standards and samples.

(1971). Samples were diluted with synthetic seawater to concentrations between 0 and 100 µM, the working range of the standards. Absorbance was measured at 6400 Å, using a 1 cm cell. The sample concentration was determined by comparison with a standard calibration curve.

Reactive phosphate concentrations were determined by the method of Murphy and Riley (1962), as described in Strickland and Parsons (1972). This method relies on the formation of a phosphomolybdate complex and its subsequent reduction to blue compounds which are measured colorimetrically through a 1 cm cell at 8850 Å. The working standards are in the range of 0 to 20 µM, requiring pore water dilutions of 1:4 and 1:8.

Reactive silicate was determined using a modified method of Mullin and Riley (1955) found in Strickland and Parsons (1972). The silicomolybdate complex which is formed is reduced to a dark blue compound and measured colorimetrically through a 1 cm cell at 8100 Å. Interstitial waters were diluted 1:10 using artificial seawater to bring the concentration into the range of the working standards, 0 to 150 µM.

Dissolved sulfate was measured by $BaSO_4$ precipitation. A 0.25 ml solution of acidified 500 mM $BaCl_2$ spiked with Ba-133 was added to 0.5 ml of sample pore water. $BaSO_4$

was separated by filtration on a Whatman Glass Fiber Filter, Grade C. The amount of $SO_4^=$ on the filter was determined by counting Ba-133 on a NaI detector with multi-channel analyzer and compared to Copenhagen Standard Sea Water with a known sulfate concentration.

Chloride concentrations were determined with a clinical chloride titrator which coulometrically titrates the chloride ions with silver ions until the end point is reached. The concentration in milliequivalents per liter was determined by comparing the time of titration to known standards.

Problems associated with interstitial water extraction procedures have been reported for PO_4^{-3} and SiO_2. Bray et al (]973) reported appreciable loss of phosphate during extraction when squeezing samples under aerobic conditions. Oxidation of Fe II to Fe III may cause direct precipitation of PO_4^{-3}, or $Fe(OH)_3$ may scavenge PO_4^{-3} after precipitation. The decrease was shown to be as great as 25 percent. Recent experiments conducted after completion of this study have shown that cores extracted and centrifuged in an inert atmosphere produced PO_4^{-3} values 50 to 100 percent higher than cores extracted and centrifuged open to the atmosphere (Hammond and Fuller, personal communication). Thus, the PO_4^{-3} data is presented with very little quantitative certainty.

Fanning and Pilson (1971) have reported a significant effect on the apparent silicate concentration when the temperature of extraction was warmer than the interstitial water temperature. For deep sea sediments, a 20° C increase in temperature produced an apparent concentration 50 percent higher than the concentration at in situ temperature. The temperature of interstitial water extraction for San Francisco Bay sediments, which ranged from 20 to 23° C, was only a few degrees warmer than the in situ temperatures, 15° to 20° C. This may have produced SiO_2 values 6 to 10% higher than true concentrations, assuming the temperature effect is linear.

Pore Water Storage

$T\text{-}CO_2$ analyses were always run immediately after extraction. Other nutrient analyses were also carried out within 2 hours after extraction on the 7/77 and 10/77 trips to San Francisco Bay, except for samples collected on the 3/77 cruise which were quick frozen in a dry ice solvent bath and stored for 2 to 6 weeks before analysis. Experiments designed to assess the impact of freezing and refrigeration on nutrient concentrations in seawater (Miller, 1977) showed dissolved silica concentrations remained the same or increased by about 5 percent, while

PO_4^{-3} showed a slight decrease of about 5 percent. The percentage gain of silica and loss of phosphate increased with each episode of freezing and thawing. Short term refrigeration showed very little change in apparent concentration for SiO_2 and PO_4^{-3}. The test did not include analyses for changes in ammonia concentration.

Pore water storage did prove to be a problem for the $SO_4^{=}$ concentration determination. Pore water $SO_4^{=}$ for several of the stations was analyzed 2 to 6 months after collection and several high values relative to the water column concentration were measured. Subsequent experiments, including chlorinity determinations, showed the high values were due in part to increased salinity resulting from evaporation (see Appendix C). In addition, some of the high $SO_4^{=}$ values, especially those for the upper intervals of South Bay cores, may have resulted from interference by dissolved organics which precipitate in acidic solutions and absorb Ba^{+2} (see Appendix C). Values used in this study have been corrected for these problems and should be accurate to within 15 percent.

X-Radiographs

X-Radiographs of the sediments were made at several stations throughout the bay to evaluate sediment struc-

tures. Cores were sliced to fit into 2 cm deep trays immediately after collection. The radiographs were taken at 50 keV using a Faxitron with automatic exposure and a source to sample distance of about 90 cm.

RESULTS

Pore Water Concentrations

In Figures 2 through 13, nutrient concentrations are plotted against depth for San Francisco Bay stations. The core numbers include the station locations (refer to Figure 1) and the date of collection. Table 3 contains observations of important or unusual features of the profiles. The shaded areas of the radon profiles shematically represent Rn-222 deficiencies from secular equilibrium with Ra-226 and are approximated at depth.

Most cores are characterized by a low concentration gradient near the surface with a higher gradient below for T-CO_2, NH_4^+, and PO_4^{-3}. The depths of the break in gradient range from 4 cm for Core 13 7/77 (Figure 3) to 45 cm for Core 14C 3/77 (Figure 4). In some cores, several of the nutrients show a minimum at or near the gradient break, as demonstrated in Core 28C 7/77 (Figure 12). Silicate commonly shows a low value near the surface with nearly uniform higher concentrations at depth. Sulfate

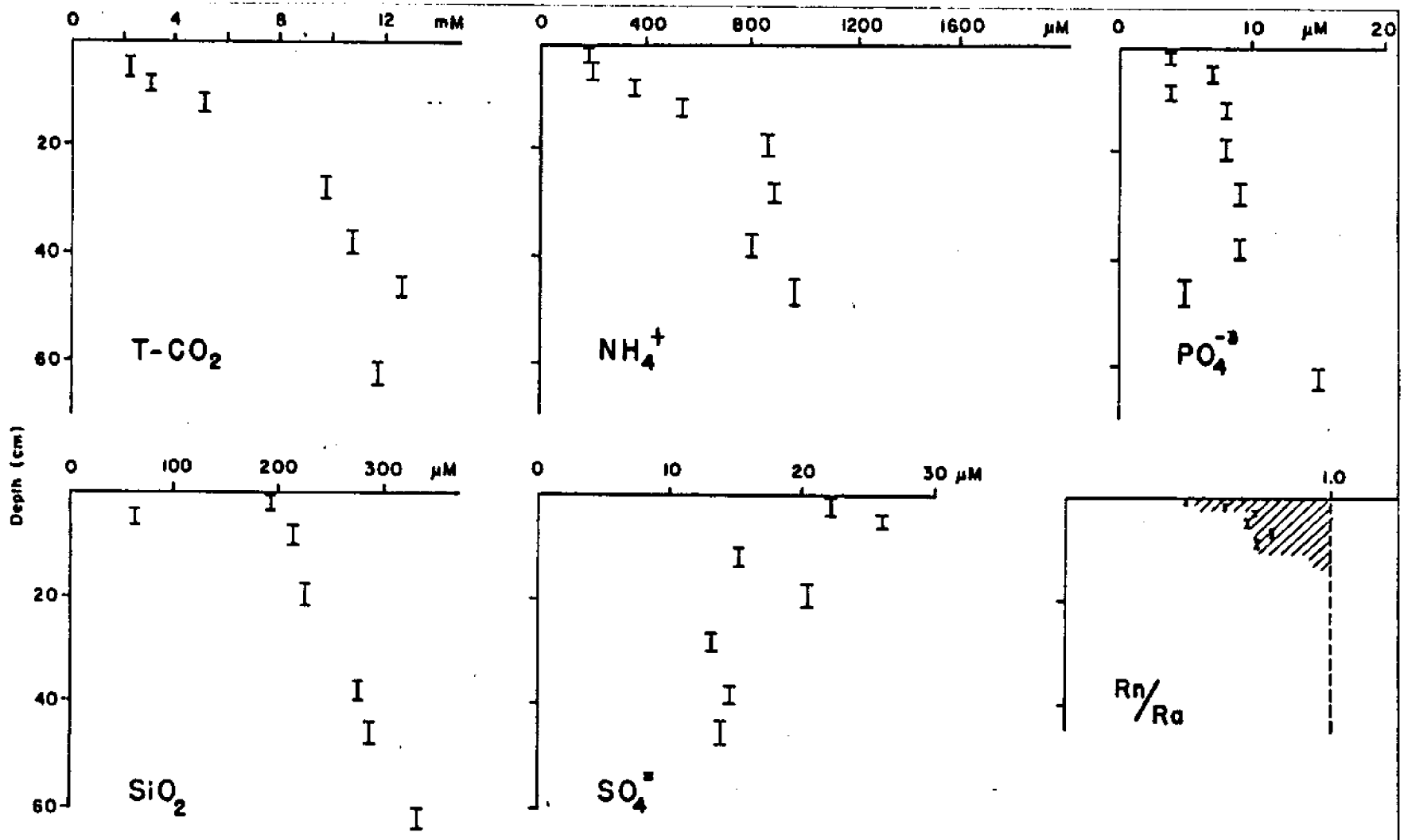

Figure 2. Nutrient Profiles for Station 13 3/77.

19

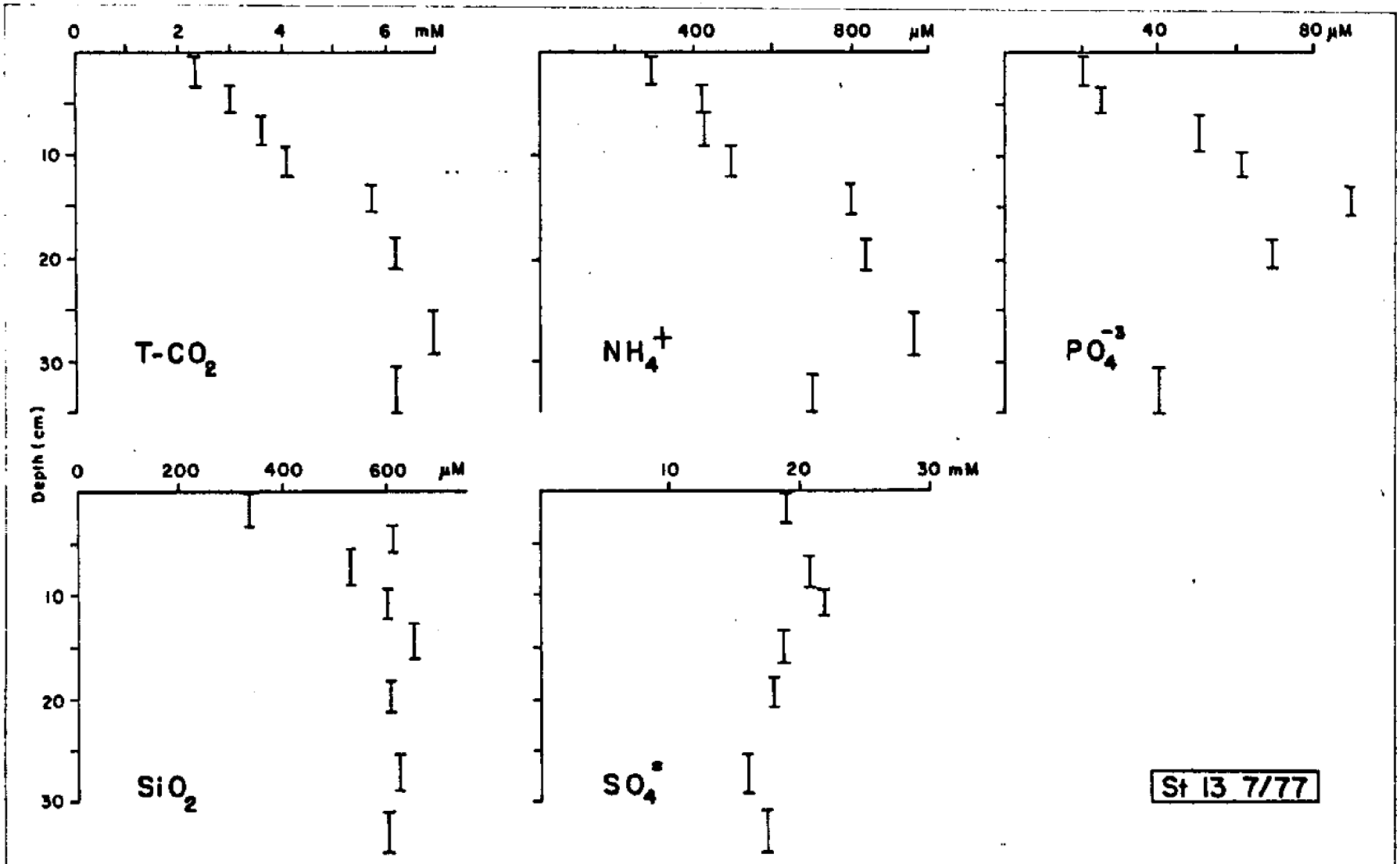

Figure 3. Nutrient Profiles for Station 13 7/77.

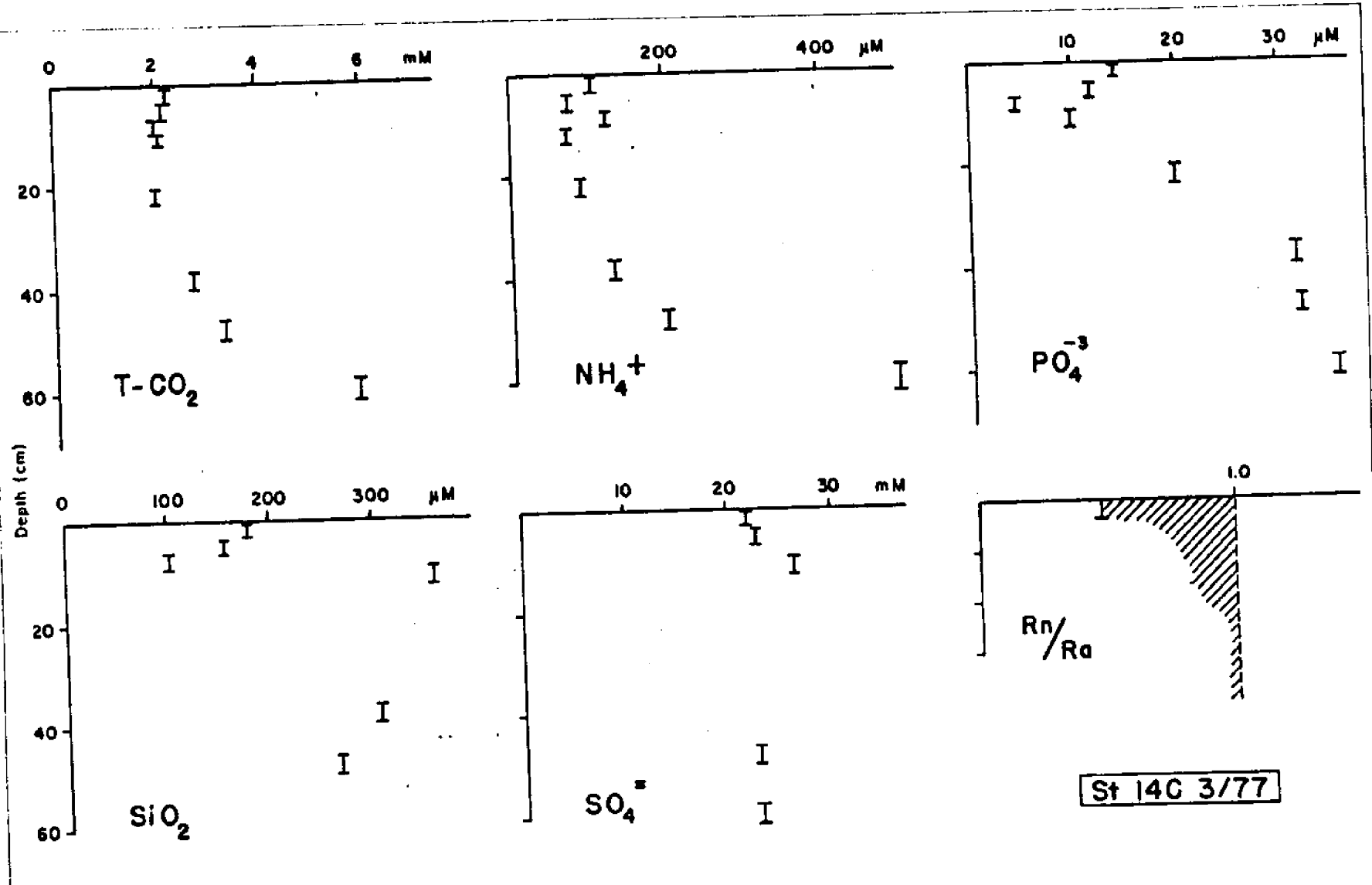

Figure 4. Nutrient Profiles for Station 14C 3/77.

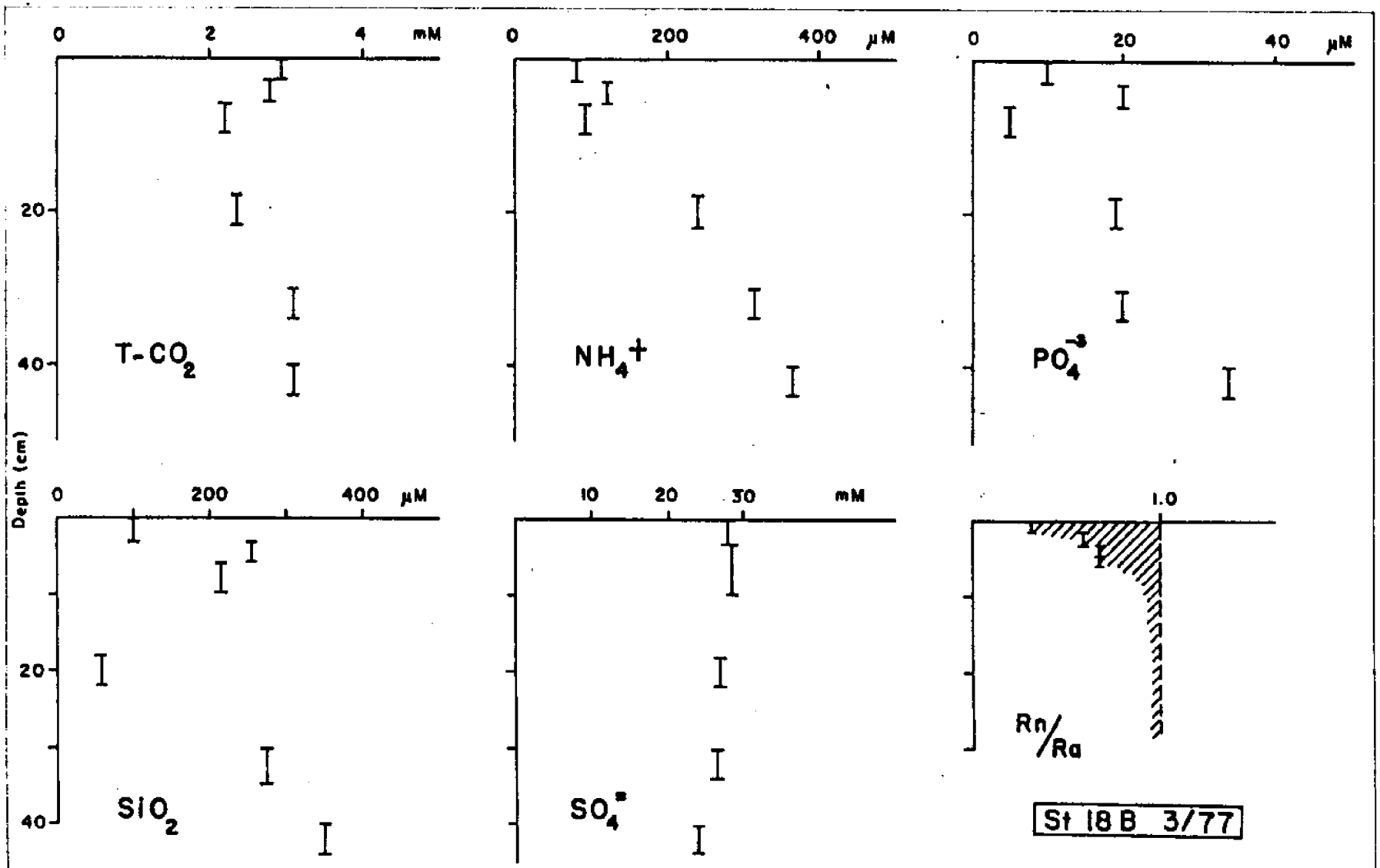

Figure 5. Nutrient Profiles for Station 18B 3/77.

22

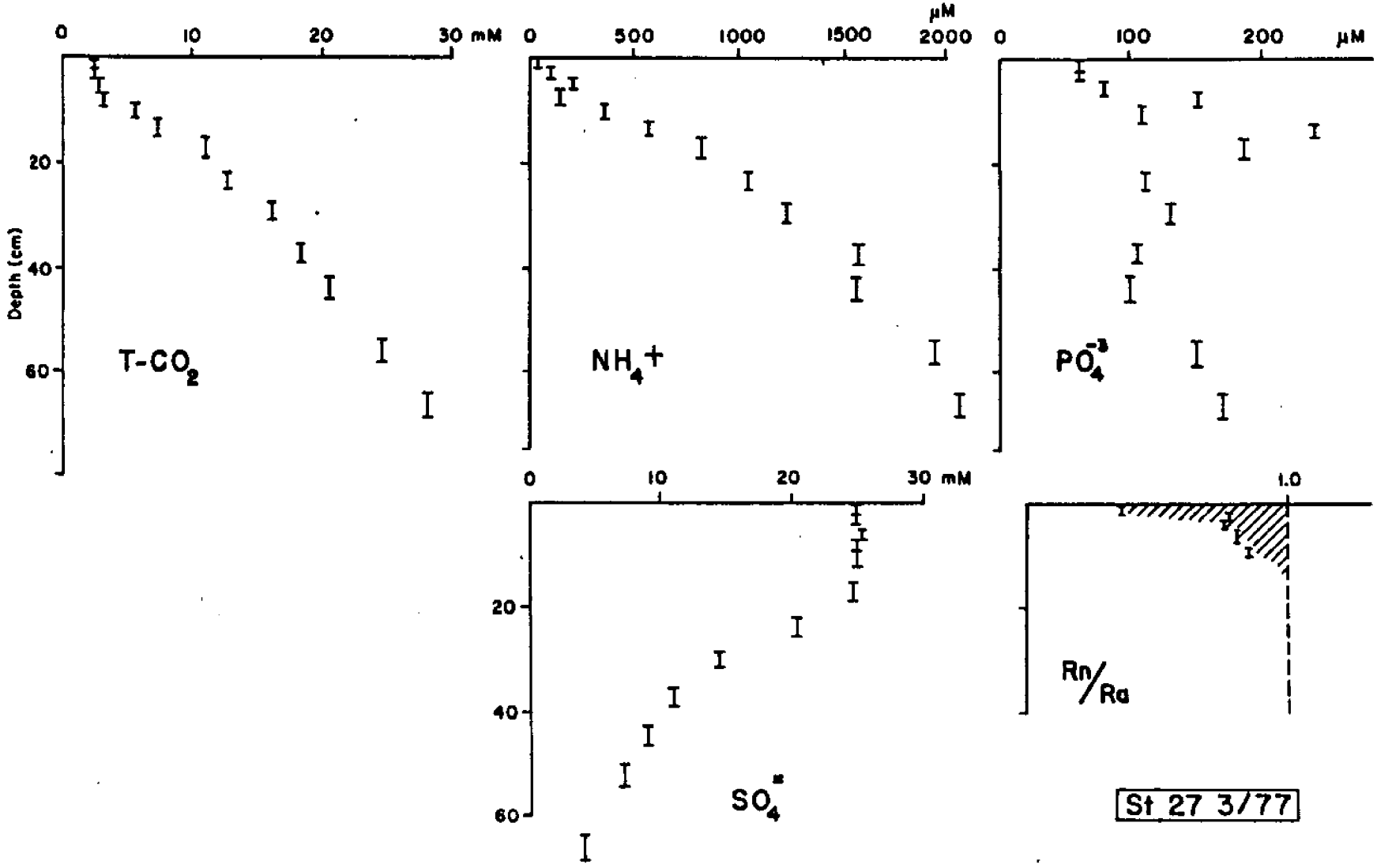

Figure 6. Nutrient Profiles for Station 27 3/77.

23

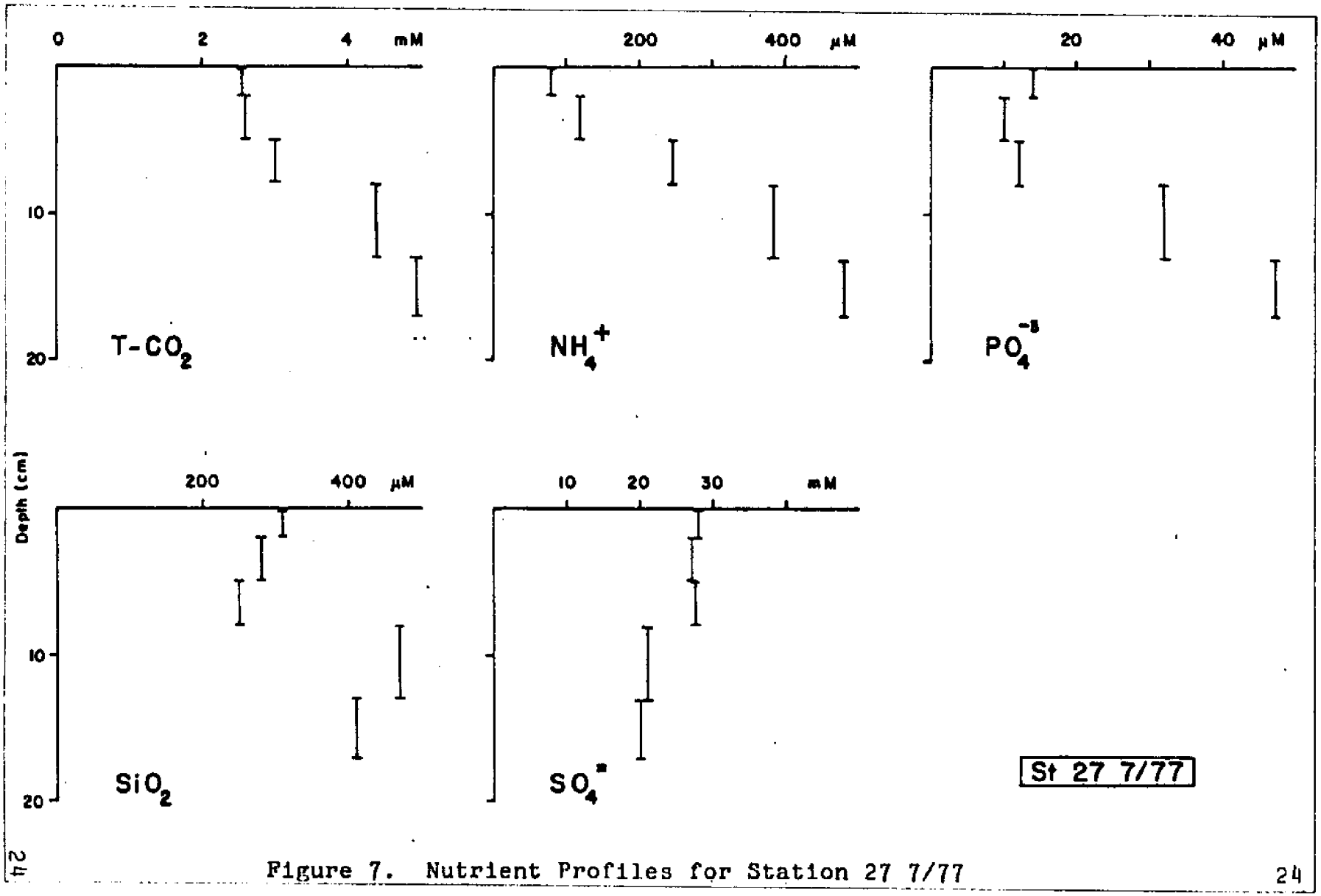

Figure 7. Nutrient Profiles for Station 27 7/77

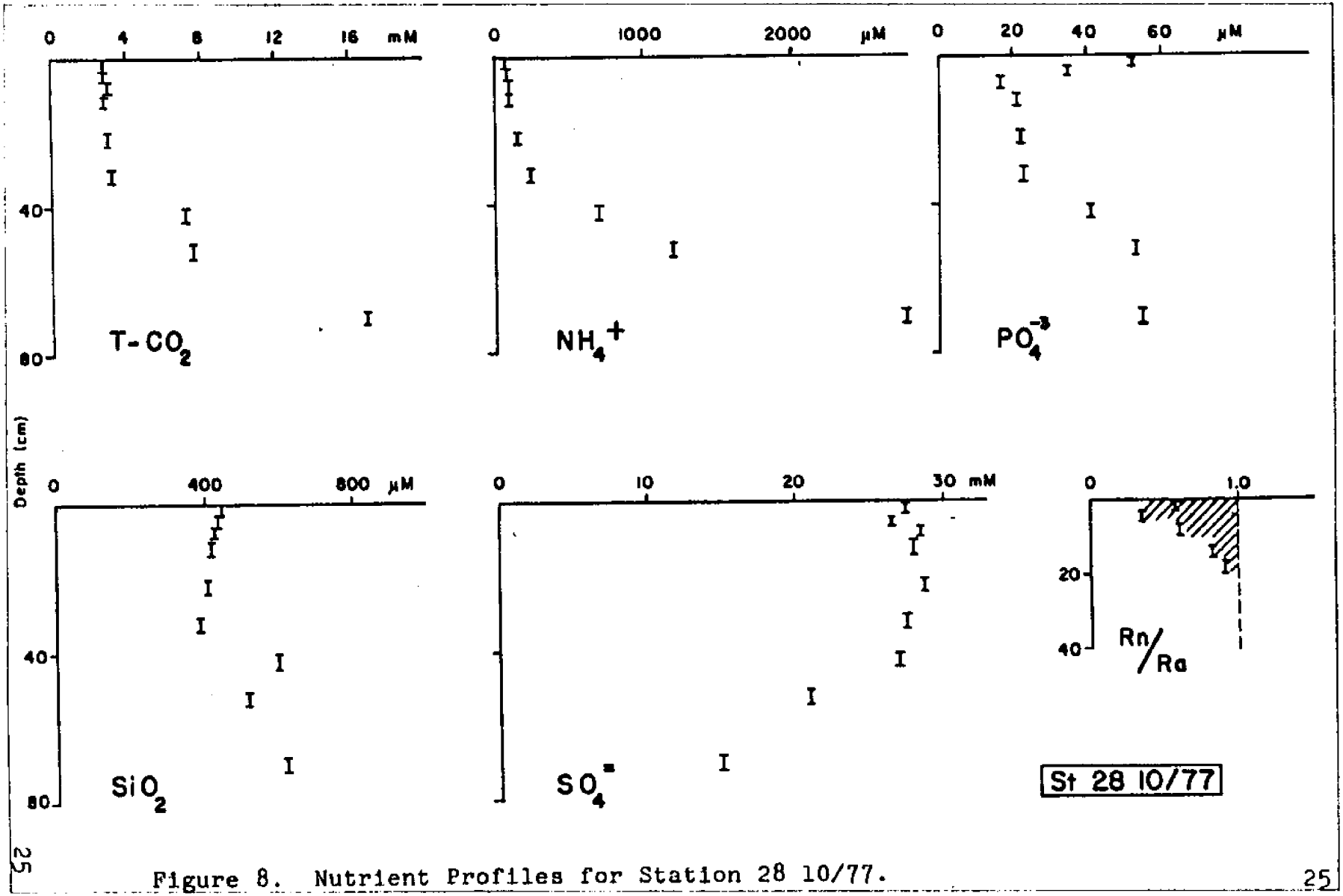

Figure 8. Nutrient Profiles for Station 28 10/77.

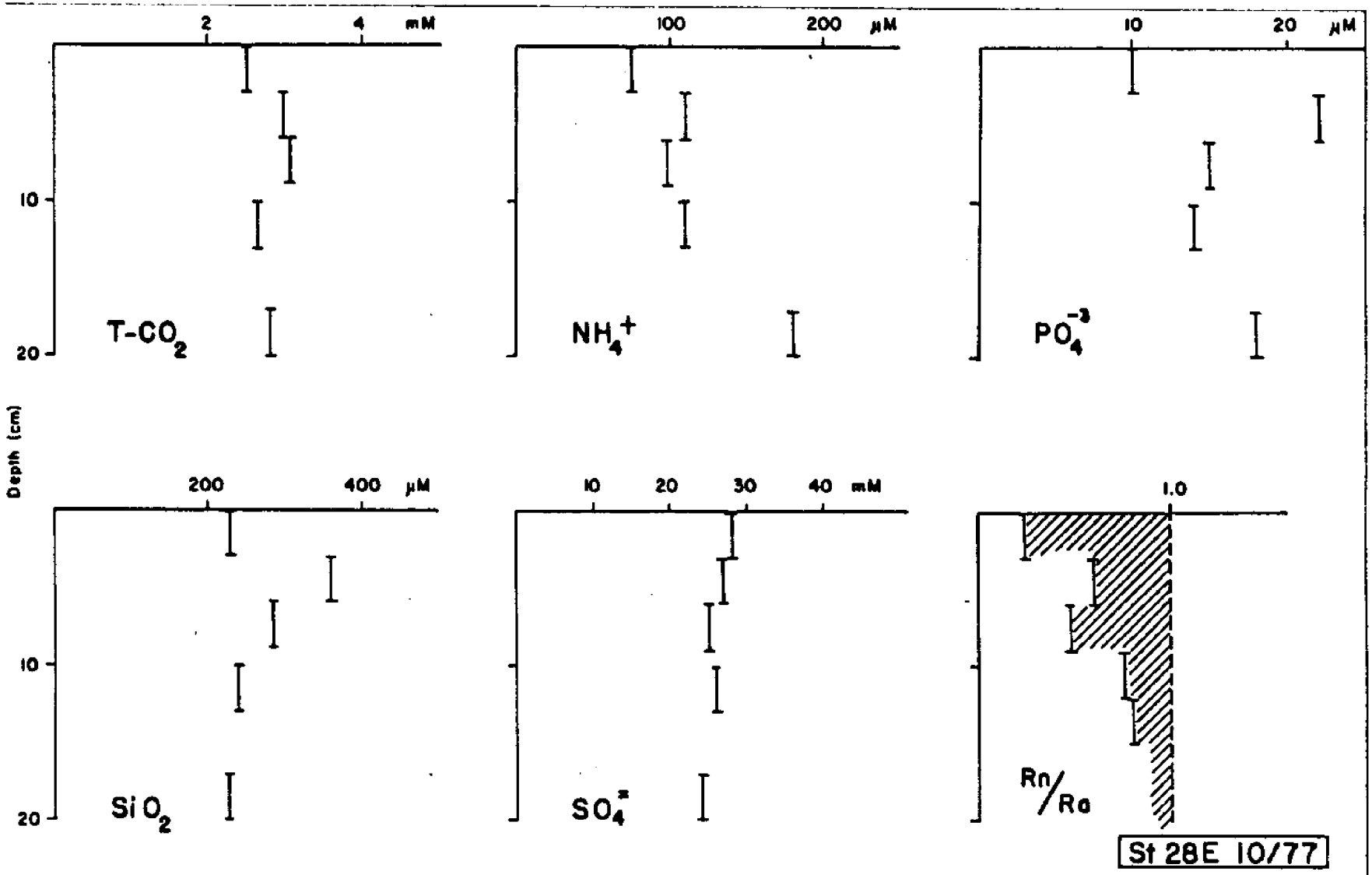

Figure 9. Nutrient Profiles for Station 28E 10/77.

26

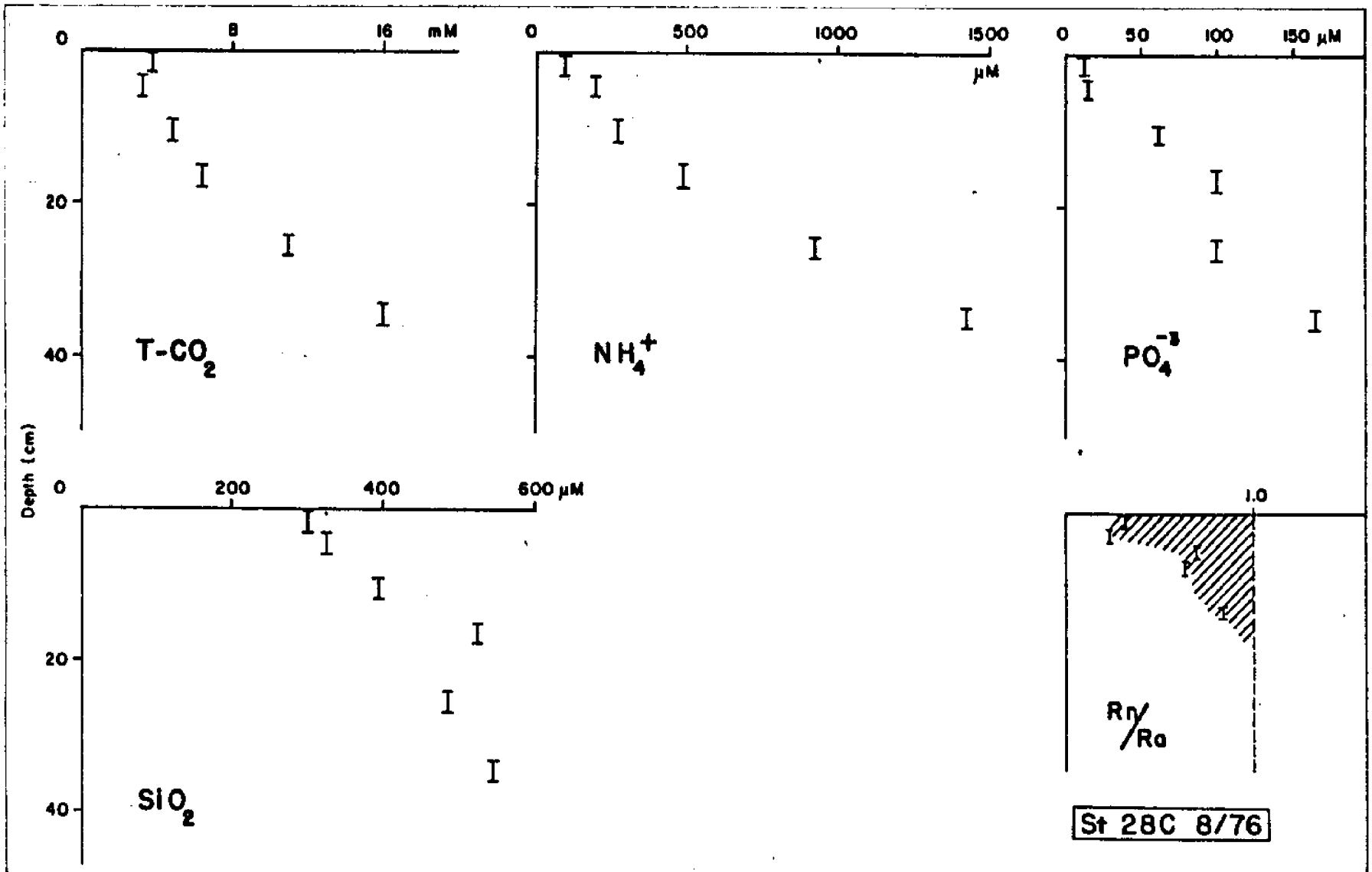

Figure 10. Nutrient Profiles for Station 28C 8/76.

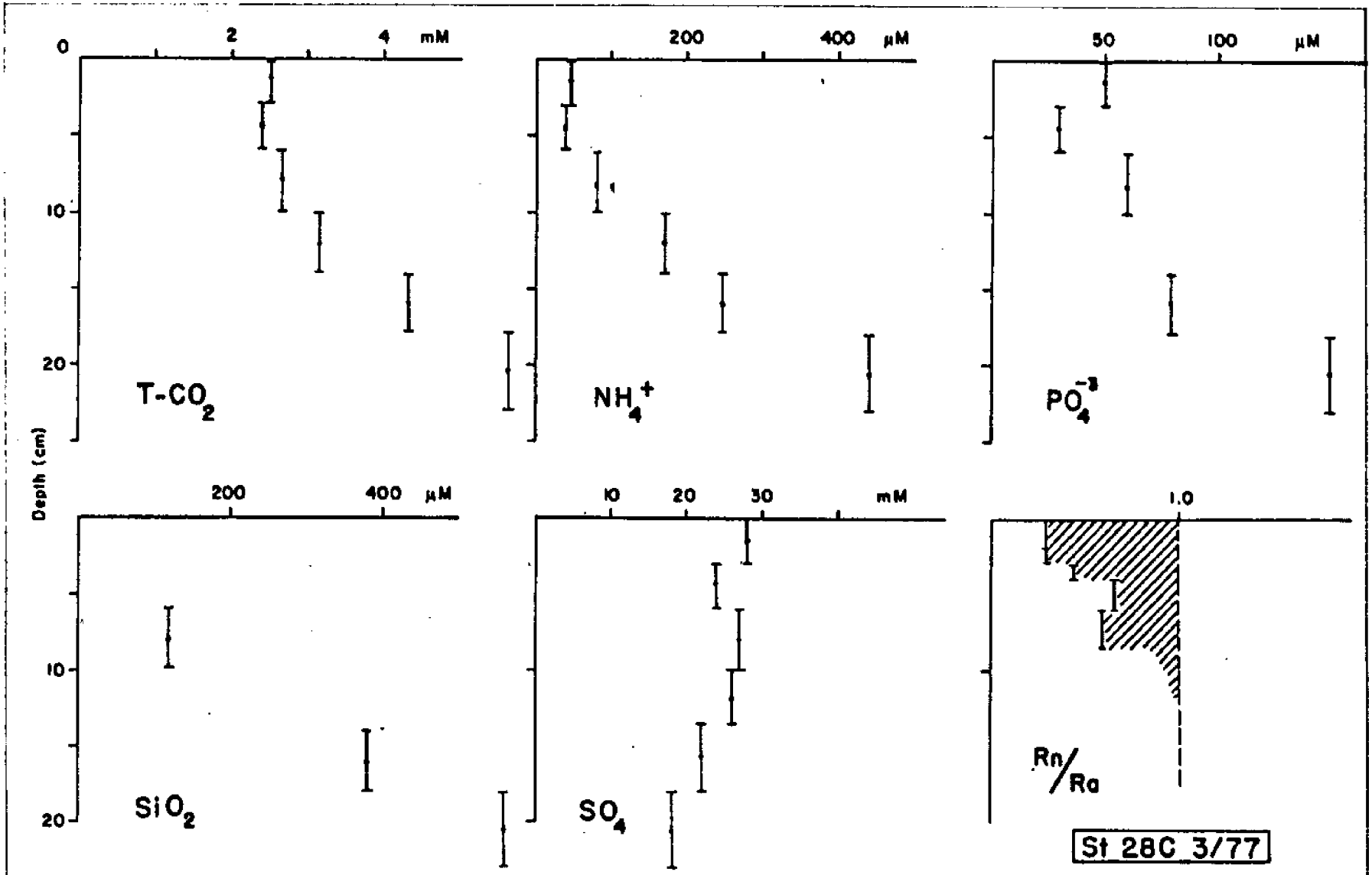

Figure 11. Nutrient Profiles for Station 28C 3/77.

28

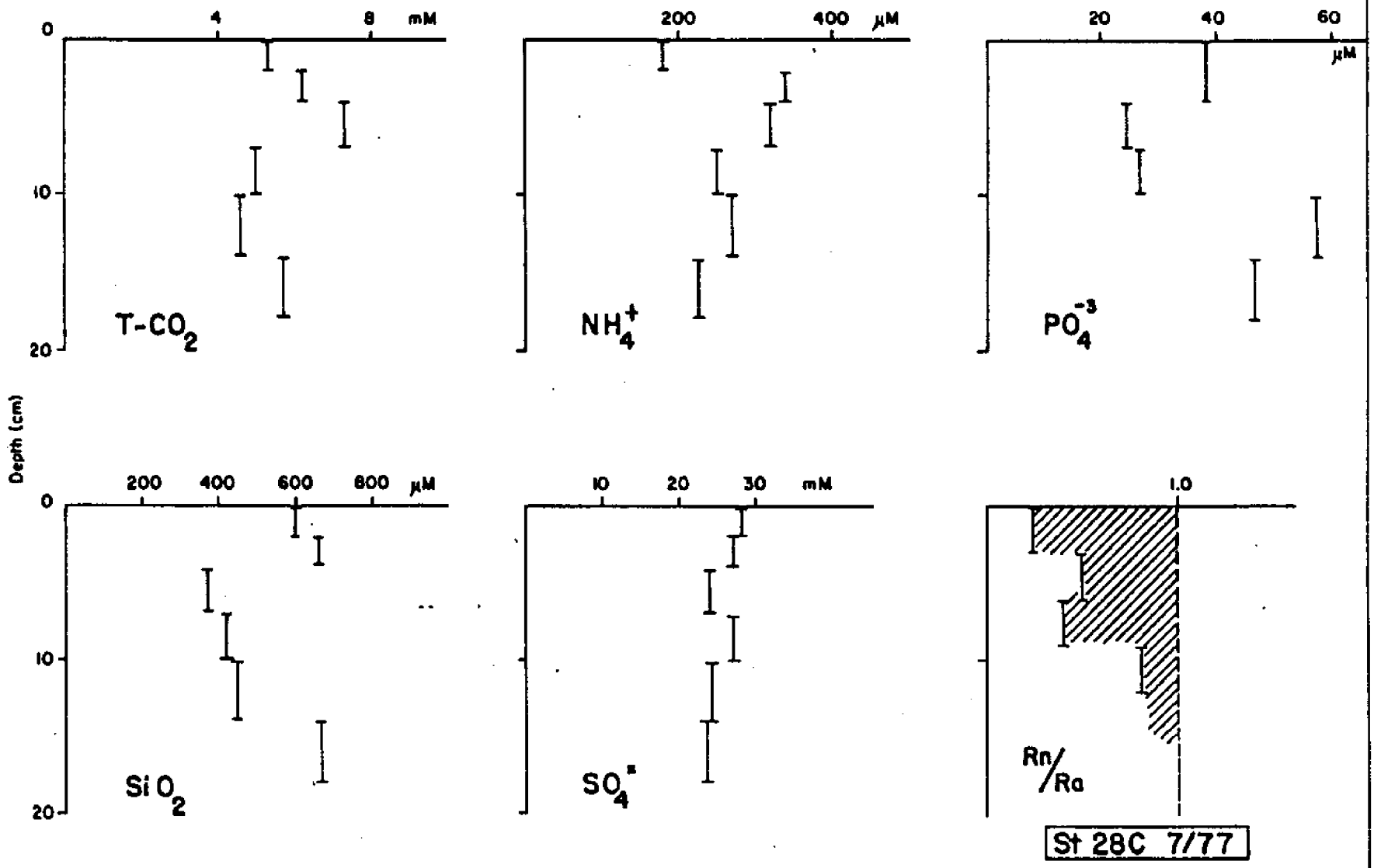

Figure 12. Nutrient Profile for Station 28C 7/77.

29

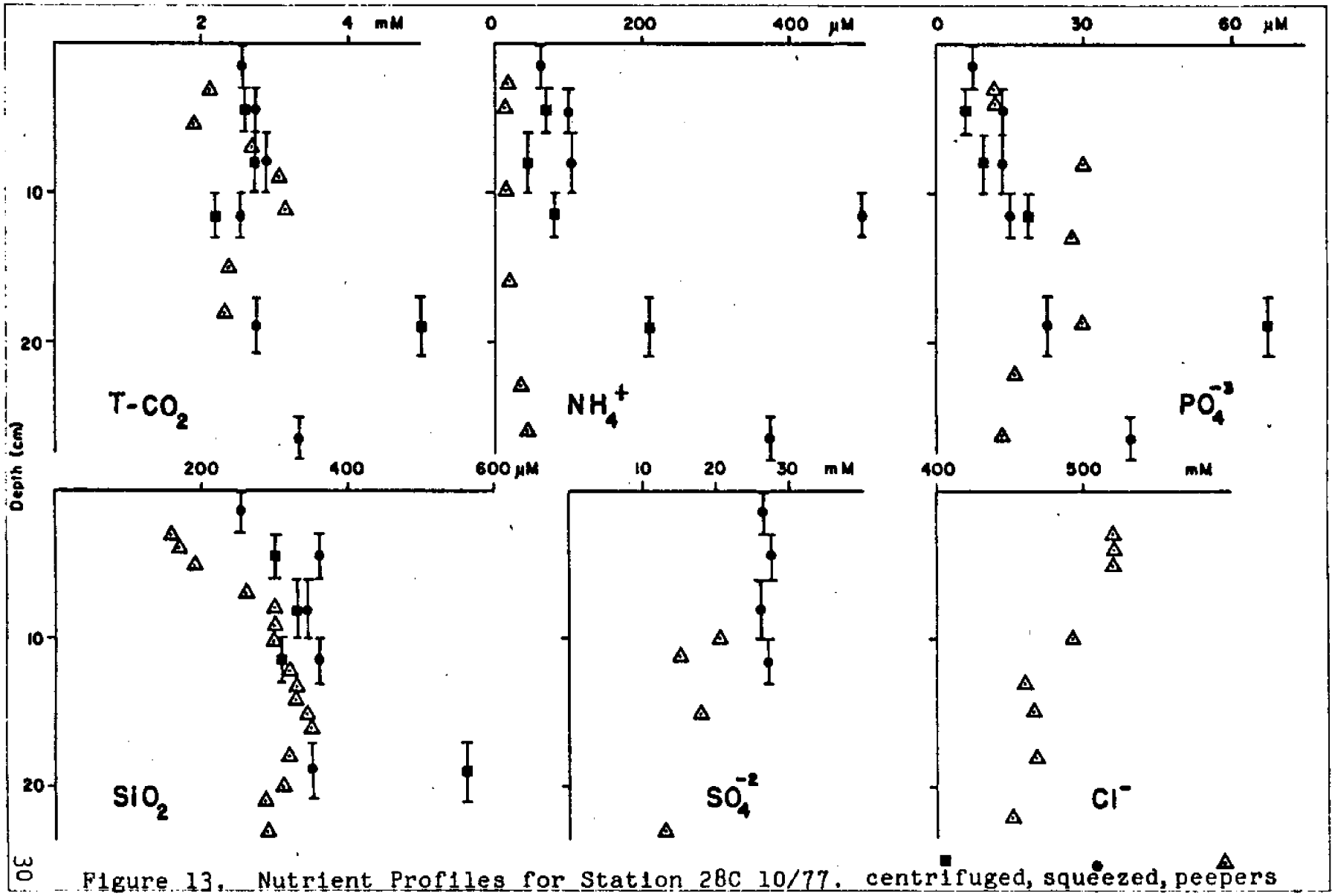

Figure 13. Nutrient Profiles for Station 28C 10/77. centrifuged, squeezed, peepers

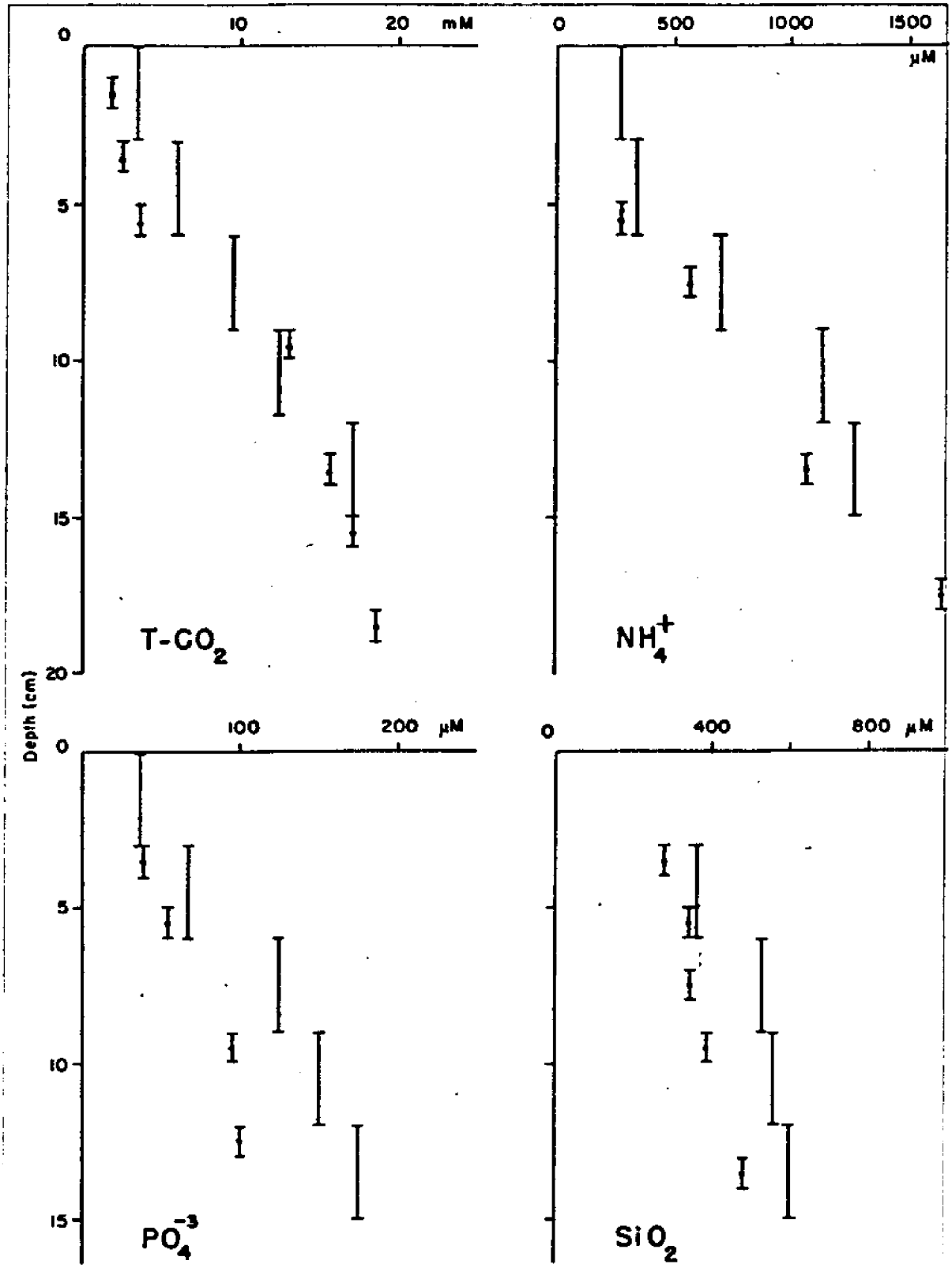

Figure 14. Nutrient Profiles for San Pedro Harbor Station 1. The shorter intervals are peeper values while the longer intervals are the average of two centrifuged cores.

TABLE 3

Features of Nutrient Profiles

Station	Feature	T-CO_2	NH_4^+	PO_4^{-3}	SiO_2	Rn
Sta 13 3/77	G	10	10	-	-	10
(WD -)	M	-	-	6-10	3-6	-
Sta 13 3/77	G	-	-	-	6-9	ND
(WD -)	M	-	-	-	6-9	ND
Sta 14C 3/77	G	40	45	20	10	ND
(WD -32)	M	21-24	9-12	6-9	6-9	ND
Sta 18B 3/77	G	-	10	40	-	10+
(WD -30)	M	6-10	6-10	6-10	18-22	-
Sta 27 3/77	G	10	10	6	-	10+
(WD -)	M	-	6-9	-	-	-
Sta 27 7/77	G	8	-	-	-	ND
(WD -)	M	-	-	2-5	5-8	ND
Sta 28 10/77	G	40	40	40	40	20+
(WD -28)	M	-	-	6-9	-	3-6
Sta 28E 10/77	G	-	20	-	-	15+
(WD -)	M	-	-	3-6*	3-6*	-
Sta 28C 8/76	G	8	-	8	-	15
(WD -ND)	M	-	-	-	-	-
Sta 28C 3/77	G	12	10	12	ND	10+
(WD -12)	M	3-6	3-6	3-6	ND	-
Sta 28C 7/77	G	-	-	-	-	12+
(WD -)	M	10-13	14-18	6-10	-	-
Sta 28C 10/77	G	12	12	12	9	ND
(WD -10)	M	10-13	6-10	-	-	ND

NOTE:
G Depth of gradient break (cm)
M Depth of minimum (cm)
- Feature not observed
* Depth of maximum (cm)
ND No Data Available
WD Depth to which live worms were observed (cm)

shows uniform concentrations in the upper intervals, with decreasing concentrations below a depth of 8 cm at Station 13 7/77 and 27 7/77 and 40 cm at Station 28 10/77.

Comparison of Techniques

Concentration vs. depth profiles for duplicate cores at Station 28C 10/77 using the different pore water extraction techniques are plotted together in Figure 13. Values at corresponding intervals vary by 10 to 50 percent for NH_4^+, PO_4^{-3}, and SiO_2, but the only consistent difference was the lower NH_4^+ values for the squeezed core. When this experiment was repeated using adjacent subcores from a boxcore taken from Santa Barbara Basin, the NH_4^+ difference was not detected. Differences noted between the two methods may be due to spatial variations in the sediments. This possibility is discussed in a following section (see Spatial Variation).

X-Radiographs

To illustrate features found in many of the X-Radiographs of sediment cores, a few examples are presented in Figure 15. Table 4 summarizes features in all radiographs. Many of the radiographs show extensive polychaete burrowing. The surface density of burrows (p_1) was determined by

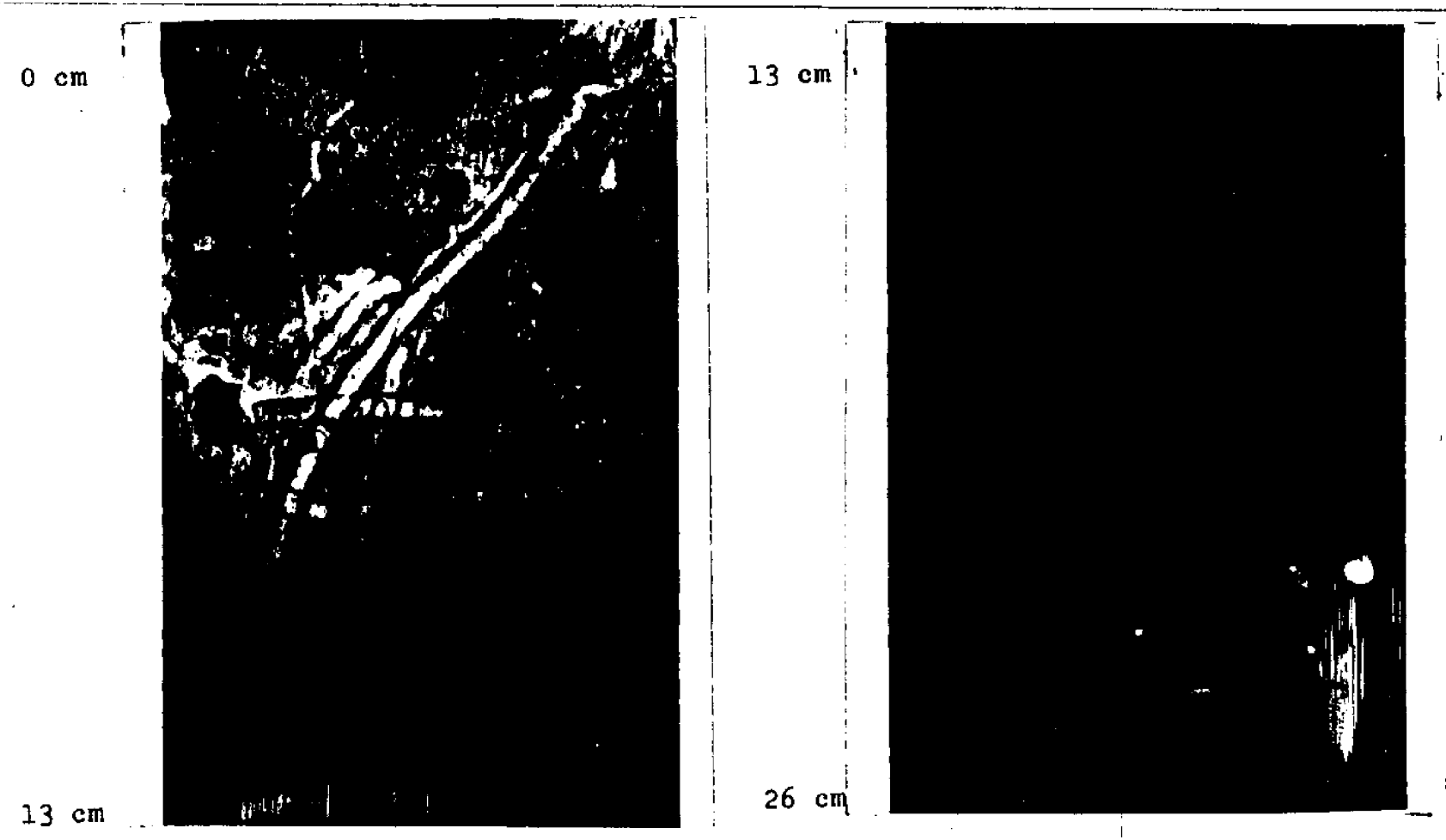

Figure 15. X-Radiographs. Sediment core for Station 20.46E from South Bay.

34

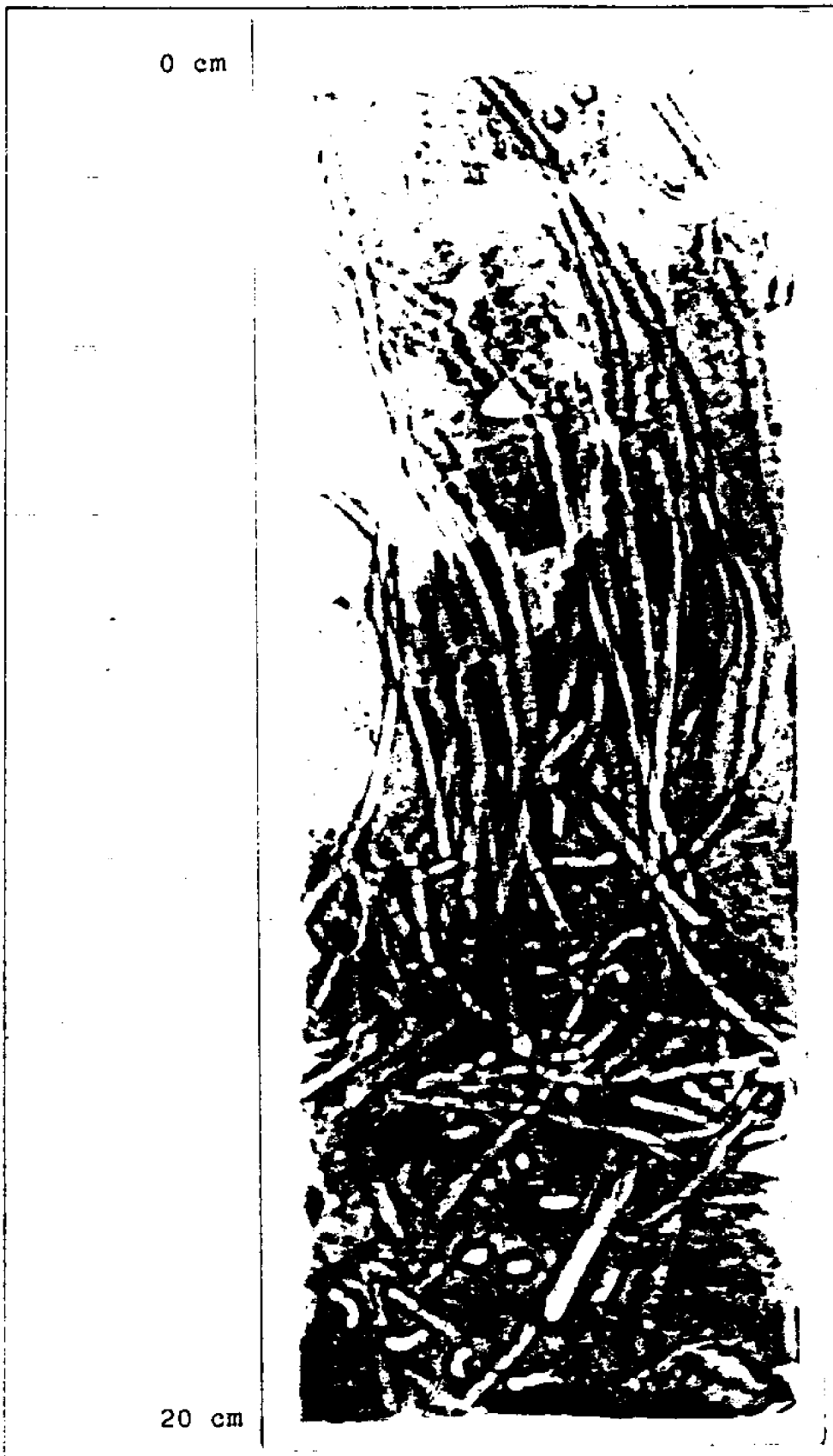

Figure 15 (Cont.) X-Radiograph. Sediment core Stat
RB2 2/78.

Figure 15 (Cont.) X-Radiograph of sediment core Station RB2 2/78.

TABLE 4

X-Radiograph Data

Station	Water* Depth (m)	P_1 (#/cm^2)	d_b (cm)	P_2 (#/cm^2)	f_w	x_b (cm)
Sta 13.22 N 2/78	4	0.31	17	0.35	3.9	1.7
Sta 14C 3/77	3	0.29	40	0.29	9.9	1.9
Sta 18 2/78	15	0.13	35	0.08	2.2	3.6
Sta 18.2 E 12/77	4.5	0.48	20	0.35	5.4	1.7
Sta RB 2 2/78	0.5	0.62	20	0.70	10.2	1.2
Sta 20.46 12/77	11.5	0.19	30	0.32	7.8	1.8
Sta 27 12/77	11.0	0.24	30	0.21	3.9	2.5
Sta 28C 3/77	0.5	0.44	17	0.70	8.6	1.2
Sta 29.3 E	2	0.35	7	0.25	1.3	2.0

X-Radiographs with no Burrows

Sta 6 12/77
Sta 13.13 2/78
Sta 26 E9 2/78
Sta 30 12/77

NOTE:

d_b Lowest depth of burrow occurrence

f_w Burrow surface area/Sediment surface area

p_1 Burrow surface density

p_2 Burrow density at depth

x_b Average distance between burrows

* Depth from MLLW

counting the number of burrows (b_s) which extend to the surface of the core, and dividing by the sediment surface area represented by the radiograph (A_r):

$$p_1 = b_s/A_r \qquad \text{Eq. 2}$$

A second parameter, the average burrow density over the upper sediment zone (p_2), was calculated by summing the lengths of the individual burrows (l_b) and dividing by the maximum depth to which burrows extend, (d_b):

$$p_2 = \frac{\Sigma l_b}{d_b \times A_r} \qquad \text{Eq. 3}$$

The surface area of these burrows was calculated by measuring the individual burrow lengths and diameters in the radiographs. By dividing the sum of the burrow surface areas by the sediment surface represented by the radiograph, a surface area ratio (f_w) is calculated.

The average distance between burrows (x_b) was calculated from the reciprocal square root of burrow density $(p_2)^{-1/2}$ and the average burrow radius (r_b):

$$x_b = p_2^{-1/2} - 2(r_b) \qquad \text{Eq. 4}$$

Spatial Variation

The two cores taken at Station 28C 10/77 were used

for a comparison of pore water extraction techniques (Figure 13). Because the average of the variations in measured concentrations were within the analytical precision, the techniques were determined to be equally useful. The differences for equivalent intervals in these cores, however, were greater than the margin of error for the chemical analysis. In addition, the mixed zone for core 28C 10/77c appeared to be about 4 cm deeper than that of core 28C 10/77s. These observed differences may represent lateral variations within the sediments.

An experiment was conducted in San Pedro Harbor, Los Angeles during February 1978 to further assess this possibility. Two cores taken within 3 meters of each other were both centrifuged to extract pore waters. The analytical results are plotted in Figure 16. Large variations were found once again, with core SPH 2/78B showing a higher gradient and higher concentrations at depth for all four species measured.

The lateral variation of pore water chemistry demonstrated by such experiments may be due to heterogeneity of sediments or distribution of the macro-benthos or bacterial activity. Several stations were cored 2 or 3 times throughout the year to determine possible seasonal differences, but the possible existence of lateral variations over short distances complicates the detection of

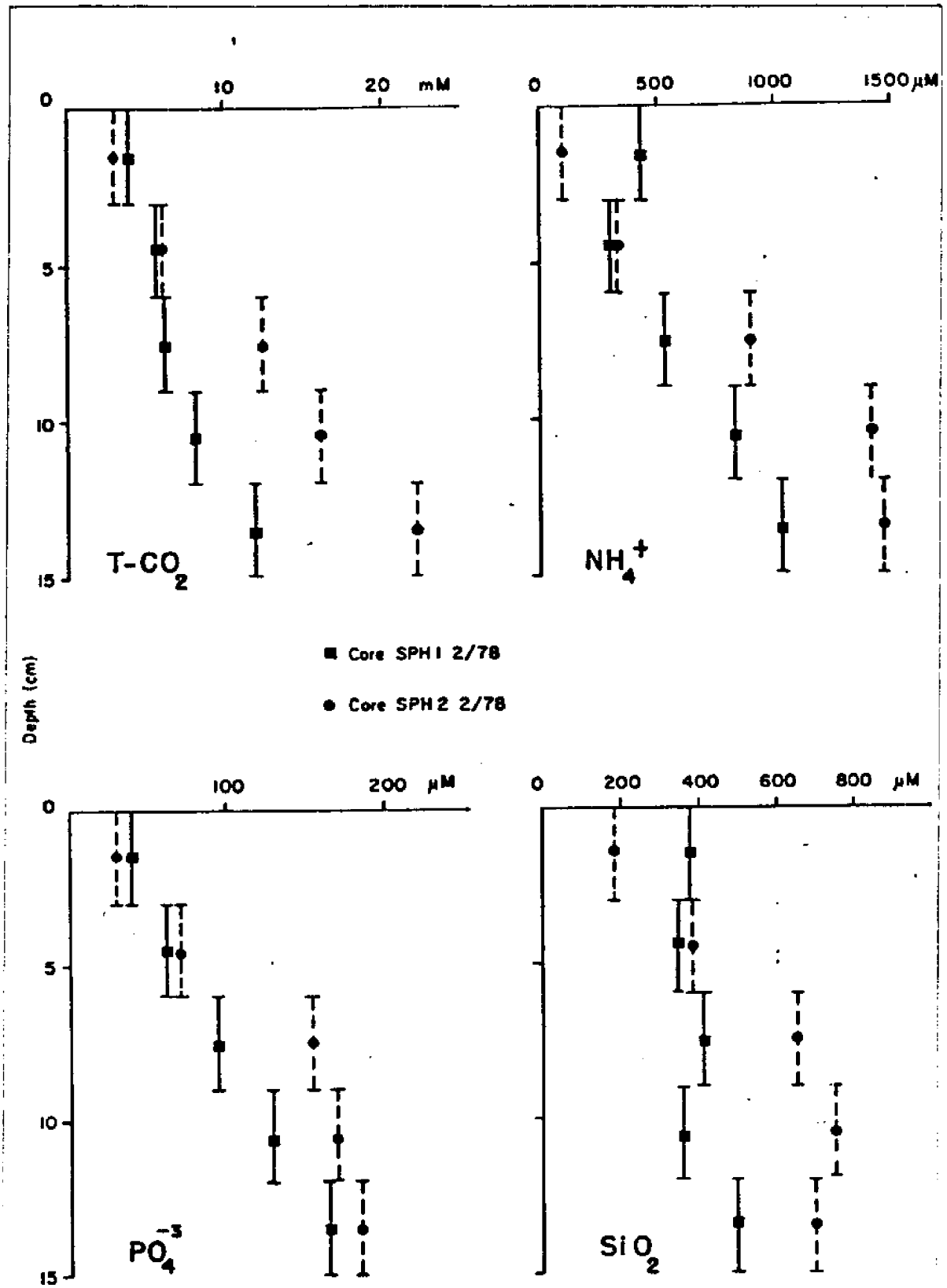

Figure 16. San Pedro Harbor Station 1 showing Spatial Variation. Both cores were centrifuged.

temporal variations. The averaging of data for several cores at the same station would be necessary to study seasonal variations.

Lateral variations suggest horizontal concentration gradients and consequent horizontal diffusion. This may be a significant process in some areas, such as the small scale horizontal gradients across worm burrow surfaces, but the larger scale horizontal variations observed between cores result in concentration gradients two to three orders of magnitude smaller than vertical gradients in the same region.

DISCUSSION

Nearly all profiles are characterized by a lower zone with linear slopes showing relatively large concentration gradients, and an upper zone with very little change of concentration with depth. The build-up of $T\text{-}CO_2$, NH_4^+, and PO_4^{-3} in the interstitial waters is due to the breakdown of organic matter aerobically near the surface and anaerobically below. The concentration gradients can be used along with diffusivities (D) to calculate fluxes through these zones from Fick's First Law. Nutrient fluxes through the lower zone resulting from molecular diffusion (J_{MDL}) are calculated as follows:

$$J_{MDL} = D_s \, (dc/dx)_L \qquad \text{Eq. 5}$$

where dc/dx_L is the lower zone concentration gradient and D_s is the coefficient of diffusion through sediments:

$$D_s = \frac{D_t \, \emptyset}{\theta^2} \qquad \text{Eq. 6}$$

D_t, the temperature dependent diffusivity in sea water, was determined from the graph in Figure 17, after Li and Gregory (1974). The porosity $\emptyset$ was estimated to be 60 to 80 percent. A value of 1.2 was estimated for the tortuosity θ (Li and Gregory, 1974). Values used for D_s are listed in Table 5.

It is uncertain what happens to the nutrient flux as it passes through the upper zone. The resulting flux across the sediment-water interface may be significantly different from the molecular diffusive flux, owing to the physical and biological processes operative in the upper zone. On the basis of nutrient profiles and sediment radiographs from San Francisco Bay, three models have been proposed to calculate the interface flux.

Model 1

Model 1 treats the sediments as a two box system, with a lower anoxic zone of molecular diffusion and an

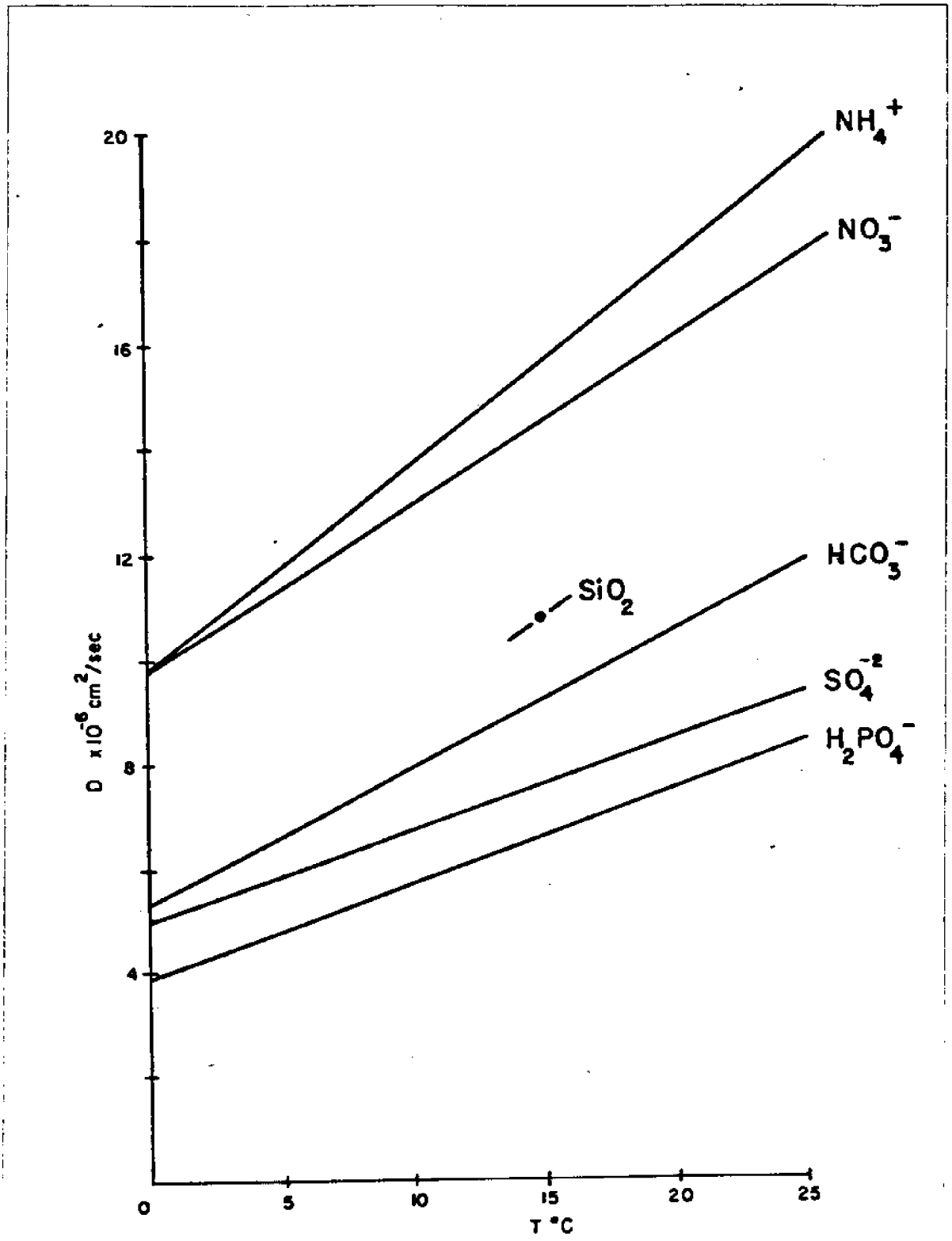

Figure 17. Coefficients of Molecular Diffusion. Determined for sea water, as a function of temperature.

upper bioturbated zone with extensive reworking of sediments by macroorganisms (see Figure 18). Burrowing and scavenging by polychaetes such as Nephyts sp., Pectinaria californiensis, Asychis elongata, and Heteromastis filiformis results in higher porosities and increases the mass transfer coefficient for dissolved species within the interstitial waters. This process may be considered to be an eddy diffusivity which creates smaller concentration gradients in the upper zone, with only a slight increase of species concentration with depth (Sta 28 10/77, Figure 8), (Goldhaber et al, 1977).

For species such as $T\text{-}CO_2$ which should not be lost through chemical reactions in the upper zone, the flux through that zone (J_U) is at least as high as the flux through the lower zone (J_{MDL}):

$$J_{MDL} = D_s \, (dc/dx)_L \quad D_{Ml} \, (dc/dx)_U = J_U \qquad \text{Eq. 7}$$

where D_s is the coefficient of molecular diffusion for the lower zone sediments, dc/dx_U is the concentration gradient for the upper zone, and D_{Ml} is an effective diffusivity for the upper zone:

$$D_{Ml} = D_s \, (dc/dx)_L \, (dc/dx)_U^{-1} \qquad \text{Eq. 8}$$

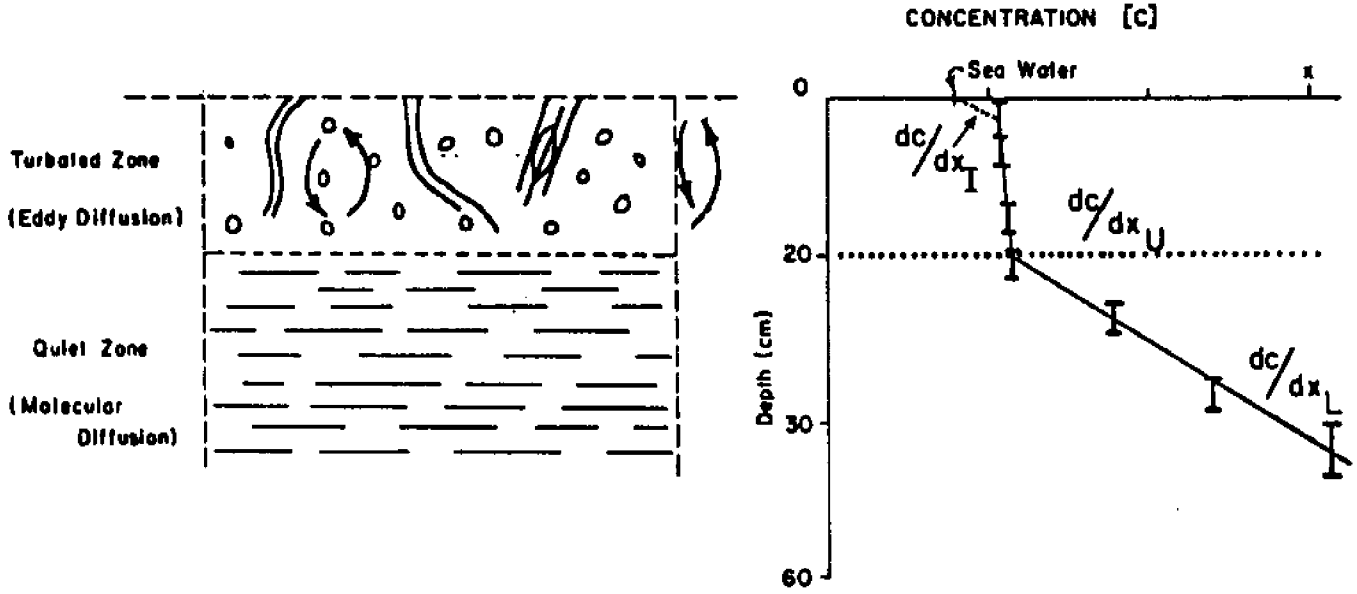

Figure 18. Model 1. Macrobiological activity in the upper zone results in eddy diffusion and relatively faster rates of mass transfer.

TABLE 5

Parameter Values

Station	$D_s(T\text{-}CO_2)^{(1)}$	$D_{M1}^{(1)}$	$D_{M1}/D_s^{(3)}$	$R^{(2)}$
Sta 13 3/77	4.1	17.6	4	1.7
Sta 13 7/77	6			
Sta 14C 3/77	4.1	36	9	
Sta 18B 3/77	4.1			3.2
Sta 27 3/77	4.1	43	10	0.6
Sta 27 7/77	6	23	4	
Sta 28 10/77	5.7	128	20	1.8
Sta 28E 10/77	5.7	14	3	1.8
Sta 28C 8/77	6		3	3.4
Sta 28C 3/77	4.1	41	10	2.8
Sta 28C 7/77	6			3.7
Sta 28C 10/77	5.7	28	5	1.8

(1) Units are 10^{-6} cm^2/sec

(2) Units are 10^{-5} cm/sec

(3) D_s of $T\text{-}CO_2$ used

D_{M1} calculated for $T\text{-}CO_2$ can be considered as a turbulent diffusivity. Assuming this value applies to the entire upper interval, it can be used with the concentration gradient across the sediment-water interface, dc/dx_I, to calculate a flux across the interface (J_{M1}):

$$J_{M1} = D_{M1} (dc/dx)_I \qquad \text{Eq. 9}$$

The interface concentration gradient is determined from the concentration of the top sediment interval and water column data. Because the top interval covers two or three centimeters depth, the pore water chemistry can only be determined as an average concentration over that interval. The measured value is assigned to the mid-point of the interval. The true gradient may be greater than this, resulting in the calculation of a minimum value for the flux.

Model 2

Nutrient profiles occasionally show minima at a depth of a few centimeters, such as for Core 28C 7/77 (Figure 12). Below the minima is a quiescent zone with steep concentration gradients. Decreased $SO_4^=$ concentrations suggest anaerobic conditions. The concentrations at the minima sometimes approach the water column concentrations for

PO_4^{-3} and SiO_2, but are usually higher for all species.

In many areas of the Bay, most notably those which are represented by Station 20, 27, 28C, 28D, and 18B, large populations of tube forming polychaetes are found. Pectinaria californiensis and Asychis elongata, for example, create undulations within their tubes which brings aerated water from the surface, flushing out old water, sediments, and fecal material to the surface. Rates of irrigation for the marine polychaetes Eupolymnia, Thelepus, and Neoamphitrite, determined by oxygen uptake studies and direct pumping measurements in vitro, range as high as 100 to 1000 ml/animal/day (Dales, 1961, and Goldhaber et al, 1977).

The pumped waters may be forced into the sediments around the tubes, causing an irrigation of the interstitial pore waters with waters from the water column above, as illustrated in Figure 19. The minima would be produced because of the horizontal input of water from the overlying water column at discrete zones corresponding to irrigation sites. If the irrigation takes place at a variety of depths in the top zone, a detectable minimum may not develop. This would explain cores at other stations which show near uniform concentrations with depth in the upper intervals.

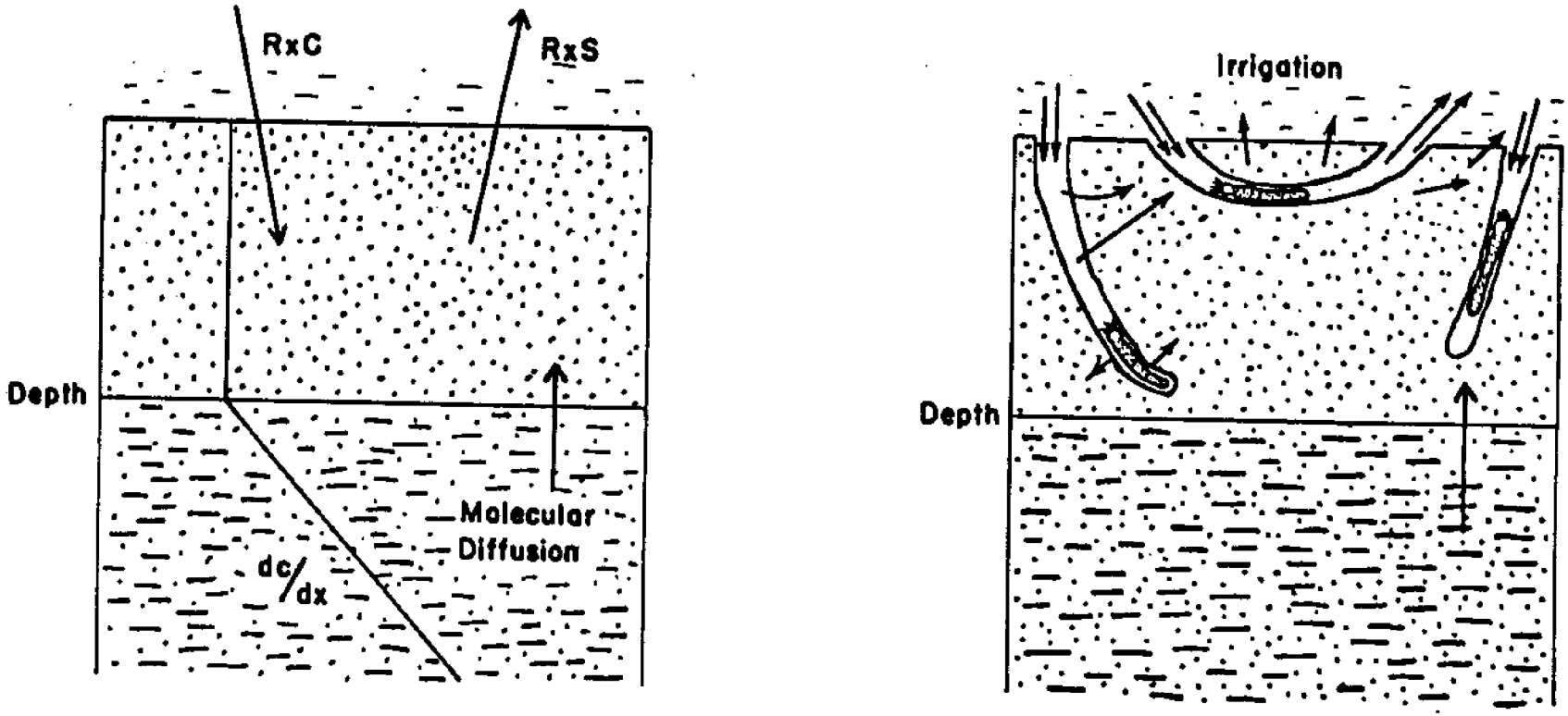

Figure 19. Model 2. Water pumped through the sediments by polychaetes increases chemical species exchange with the overlying water. Model 2 treats this irrigation as an advective process.

If the rate of water pumping can be determined (the water flux due to polychaete pumping), and the upper zone is assumed to be well mixed, a flux of nutrients can be calculated (J_{M2}):

$$J_{M2} = R\ C_{IW} - R\ C_{WC} + J_{MDI} \qquad \text{Eq. 10}$$

where R is the water pumping rate (distance/time), C_{IW} is the average concentration of dissolved species within the interstitial waters of the mixed upper zone, and C_{WC} is the dissolved species concentration for the water column. To determine a total flux from the sediments with this model, the contribution due to molecular diffusion across the sediment-water interface (J_{MDI}) is added:

$$J_{MDI} = D_s\ (dc/dx)_I \qquad \text{Eq. 11}$$

The rate of pumping (R) can be calculated if a substance with well known production rates can be identified. Radon-222, an inert gas with a 4-day half life, has proven to be a useful tracer for this purpose (Hammond and Fuller, 1978). Rn-222 is produced primarily from radium-226 within the sediments. Rn-222 and Ra-226 are in secular equilibrium over most of the deep zone of the sediments. The top zone of these sediments, however, shows a radon deficiency

greater than that expected from a simple molecular diffusive model. The Rn flux due to pumping alone (J_{RnP}) can be calculated as follows:

$$J_{RnP} = R \times S_U = I - J_{MDRn} \qquad \text{Eq. 12}$$

where S_U is the concentration of Rn-222 in the upper zone in atoms/volume, J_{MDRn} is the net molecular diffusive flux of Rn-222 out of the sediments, and I is the depth integrated Rn-222 deficiency per area in activity units:

$$I = (P \times h) - \lambda \int_0^h S \; dh \qquad \text{Eq. 13}$$

P is the production rate of Rn-222 from Ra-226 per unit volume, λ is the decay constant for Rn-222, and h is the depth to which the deficiency can be detected. Thus, the pumping rate R expressed as a velocity is determined as:

$$R = \frac{(P \times h) - \lambda \int_0^h S \; dh - J_{MDRn}}{S_U} \qquad \text{Eq. 14}$$

Values of R calculated for several of the cores can be found in Table 5. The values range from 0.6 to 3.7 x 10^{-5} cm/sec, with an average of about 2 x 10^{-5} cm/sec. Using an average worm burrow diameter of 0.25 cm and an areal density of 0.5 burrows/cm^2 determined from Equation 2, an

average R value of 2×10^{-5} cm/sec corresponds to a pumping rate of about 20 ml/animal/day if all burrows are active. This calculation, however, assumes perfect mixing of water in the irrigated zone and is consequently a lower limit for irrigation rates. The actual pumping rate of mixed waters may approach 100 ml/animal/day or more as reported by Dales (1961).

Model 3

X-Radiographs show the upper zone of many of the cores to be riddled with polychaete burrows. Assuming that these burrows are occupied, with rapid irrigation and water exchange, the molecular diffusive flux from the sediments would be increased because these burrows increase the surface area of the sediments exposed to estuarine waters (Figure 20).

The burrow surface area per area of sediment bottom (f_w) ranged from 2 to 15. The flux resulting from this increased surface area (J_{M3}) is:

$$J_{M3} = D_s \, (dc/dx)_3 \times f_w \qquad \text{Eq. 15}$$

where D_s is the coefficient of molecular diffusion for upper zone sediments and dc/dx_3 is an average concentration gradient normal to the burrow surface. Samples analyzed

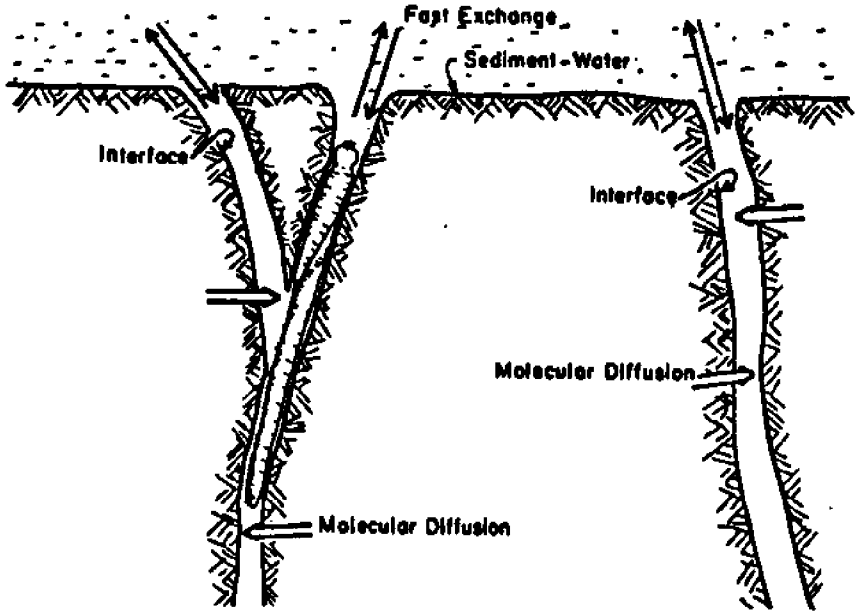

Figure 20. Model 3. Polychaete burrowing increases the area over which molecular diffusion can occur.

53

would be a mixture of tube water which would have a chemistry similar to the overlying water, and true interstitial water. If the worm burrows make up 3 percent of the volume of the upper sediments, and all this water is extracted preferentially during centrifugation, the average total of 12 ml of water extracted from a 3 cm interval is 12 percent burrow water and 88 percent true pore water. The measured concentrations must therefore be corrected to the true interstitial water concentration, c', and the gradient becomes:

$$dc/dx_3 = \frac{2\ (c' - c_w)}{x_b} \qquad \text{Eq. 16}$$

where c_w is the average water column value and x_b is the average distance between burrows calculated in Equation 4.

Model Limitations

The actual concentration gradient across the sediment-water interface is likely to be higher than the average concentration gradient over the first 3 cm of sediments, dc/dx_I, which is used in Model 1. This may result in the calculation of lower limit values. This model also assumes that no reactions take place throughout the upper sediment zone, while it is likely that aerobic oxidation of organics proceeds. If a profile shows a minimum for

$T\text{-}CO_2$, Model I cannot be used.

The advective processes predicted by Model 2 are physically realistic and supported by the observed minima in nutrient profiles. The application of the model in this study, however, did encounter problems. Because radon cores were often abbreviated above the zone of secular equilibrium, minimum radon deficiencies (I) were measured. This results in the calculation of lower pumping rates (R) and consequently lower fluxes.

Model 3 is perhaps the most physically realistic of the models in theory. Its application, however, greatly simplifies the problem of a complex 3-dimensional diffusive process by using averaged parameters, such as the concentration gradient dc/dx_3, and reducing terms to a 1-dimensional horizontal model. In addition, much uncertainty exists in determining the percentage of burrows with active organisms in an area from the radiographs and the rate of water circulation within the burrows. Aller and Yingst (1978) provide a detailed study of the biogeochemistry involved during exchange across the tube-sediment interface.

Model Flux Comparisons

The model fluxes calculated for each station are

listed in Table 6, expressed as mMol/m^2/day. A wide range of values are observed for each model and from station to station, with no consistent seasonal or geographical trends.

The average fluxes calculated for each model are listed in Table 7. Model 1 and Model 2 fluxes show agreement within 15 percent. The Model 3 fluxes are 30 percent greater than the other model values for T-CO_2 and SiO_2, and about 150 percent greater for NH_4^+ and PO_4^{-3}.

The average values calculated for species fluxes into the benthic chambers at South Bay stations are listed in Table 7. These values have been adjusted for respiration and photosynthesis within the chambers. The T-CO_2 values were determined from O_2 measurements, assuming the flux of O_2 out of the chamber equals the CO_2 flux into the chamber. All chamber experiments were conducted at Station 28C and 28E in South Bay, and therefore can be compared to model fluxes calculated for only these stations. Model T-CO_2 values are higher than the Bay average at these stations, ranging from 5 to 16 mMol/m^2/day,

but are under the average chamber values by about 50 percent. The average chamber values for NH_4^+, PO_4^{-3}, and SiO_2 are closer to South Bay model fluxes, but are lower by about 25 percent.

Lateral variations between exact experimental sites at a station location have been shown to occur, and may account for some of the differences.

While average model and chamber fluxes differ by 25 to 50 percent, their average values still fall within the large standard deviations (noted in Table 7) which result from the averaging of the individual flux calculations. Consequently, on the basis of this information, a superior model cannot be determined. Because of the relatively good agreement, however, all models have been judged to be reasonable means by which fluxes from turbated estuarine sediments may be approximated. A Bay-wide average of species fluxes from the sediments of the San Francisco estuarine system was approximated by averaging together individual fluxes for all models, giving values of 10 ± 6.7, 2.3 ± 3, 0.2 ± 0.3, and 5 ± 3.6 mMol/m^2/day for $T\text{-}CO_2$, NH_4^+, PO_4^{-3}, and SiO_2 respectively.

TABLE 6

Model Fluxes Across the Interface (mMol/m^2/day)

Station	Model	T-CO_2	NH_4^+	PO_4^{-3}	SiO_2
Sta 13 3/77	MDI	2.0	0.4	0.02	0.01
	M 1	4.2	1.9	0.04	1.2
	M 2	6.8	3.5	-	2.5
	M 3	7.5	6.5	0.01	3.7
Sta 14C 3/77	MDI	0.8	0.17	0.003	0.35
	M 1	6.9	2.1	0.21	3.1
	M 3	15.3	8.8	0.27	5.9
Sta 13 7/77	MDI	1.2	0.26	0.03	0.17
	M 1	1.6	0.9	0.04	1.5
Sta 18B 3/77	MDI	1.8	0.35	0.002	0.24
	M 2	22	2.3	0.15	4.3
	M 3	5.3	1.0	0.05	2.5
Sta 27 3/77	MDI	2.2	0.37	0.02	-
	M 1	13.8	1.47	0.52	-
	M 2	3.2	0.6	0.36	3.9
Sta 27 7/77	MDI	1.6	0.26	0.02	0.17
	M 1	6.9	1.9	0.03	2.6
	M 2	8.1	2.5	0.04	4.2
Sta 28 10/77	MDI	2.2	0.6	0.01	0.04
	M 1	32	5.3	0.73	24
	M 2	10	1.8	0.25	6.5
Sta 28E 10/77	MDI	0.5	0.36	0.007	0.45
	M 2	9.2	1.8	0.10	3.0
Sta 28C 8/76	MDI	4.8	0.56	0.001	0.76
	M 2	45	3.5	0.095	6.7
Sta 28C 3/77	MDI	1.1	0.2	0.022	0.17
	M 1	9.5	0.7	0.71	-
	M 2	7.3	1.1	1.0	4.6
	M 3	16.3	3.5	1.5	11.4

(Continued next page)

TABLE 6 (Cont.)

Station	Model	T-CO_2	NH_4^+	PO_4^{-3}	SiO_2
Sta 28C 7/77	MDI	2.1	0.3	0.02	0.17
	M 2	11.2	0.9	0.7	19
Sta 28C 10/77c	MDI	0.4	0.16	0.01	0.16
	M 1	4.0	0.73	0.03	2.0
	M 2	8.6	1.7	0.05	4.7
Sta 28C 10/77s	MDI	1.0	0.16	0.02	0.17
	M 1	5.4	0.96	0.04	3.2
	M 2	7.3	1.4	0.05	5.3

NOTE:
MDI Molecular diffusive flux across the interface

M 1 Model 1 flux

M 2 Model 2 flux

M 3 Model 3 flux

TABLE 7

Average Fluxes Calculated from the Models and Chambers*

(Values are mMol/m^2/day ± the Standard Deviation)

Model	T-CO_2	NH_4^+	PO_4^{-3}	SiO_2
Molecular Diffusion (Lower Zone)	1.2 ± 1.0	0.2 ± 0.12	0.012 ± .008	0.16 ± 0.10
Molecular Diffusion (Interface)	1.4 ± 0.7	0.3 ± 0.14	0.02 ± 0.01	0.24 ± 0.21
Model 1	8 ± 4	1.7 ± 1.4	0.18 ± 0.13	4.4 ± 0.8
Model 2	9 ± 5	1.9 ± 1.0	0.19 ± 0.18	4.5 ± 1.3
Model 3	11 ± 5	4.6 ± 3.2	0.46 ± 0.6	5.9 ± 4.0
Chambers	23 ± 9 1/	1.5 ± 0.8	0.2 ± 0.1	5.2 ± 1.5
Sta 28 C & E 3/ (Model 1)	6.3 ± 2.8	0.79 ± 0.14	0.26 ± 0.38	2.6 ± 0.8
Sta 28 C & E 4/ (Model 2)	14.8 ± 14	1.7 ± 0.9	0.33 ± 0.3	7.2 ± 5.8
Sta 28 C 5/ (Model 3)	16.3	3.5	1.5	11.4
Model Average	10 ± 6.7	2.3 ± 3	0.2 ± 0.3	5 ± 3.6

NOTE:

1/ Determined from O_2 measurements (Hammond, 1977) assuming flux of O_2 out of the chamber equals CO_2 flux into chamber.

TABLE 7 (Cont.)

2/ The negative values for NO_3^{-2} represent fluxes into the sediments.

3/ Stations 28C 3/77, 28C 10/77c, 28C 10/77s.

4/ Stations 28C 8/76, 28C 3/77, 28C 10/77c, 28C 10/77s, 28E 10/77.

5/ Station 28C 3/77.

6/ Weighted average of all calculated model fluxes (dominated by Models 1 and 2).

* All chamber experiments were conducted in South Bay (Station 28C and 28E) and therefore can be compared to model fluxes calculated for these stations only.

Model fluxes across the sediment-water interface are typically 6 to 10 times greater than molecular diffusive flux out of the lower zone. This suggests greater rates of organic material breakdown and nutrient regeneration in the upper mixed zone of the sediments. The calculated molecular diffusive flux across the interface does not reflect this, giving values nearly an order of magnitude lower than model and chamber fluxes. This indicates that one dimensional molecular diffusive models are inappropriate for systems with a mixed upper sediment zone.

Flux Stoichiometry

The model flux ratios of T-CO_2 : NH_4^+ : PO_4^{-3} : SiO_2 have been calculated and compared with the ratio observed for C:N:P in marine plankton, 100 : 15.1 : 0.94, with a N:P ratio of 16 (Redfield et al, 1963). The results are listed in Table 8. For all ratios, the NO_3^- nitrogen fluxes were left out. Nitrification of NH_4^+ in the upper zone may be occurring, but the observance of NO_3^- fluxes into, rather than out of the sediments during benthic chamber flux experiments at San Francisco Bay suggests that denitrification is the dominent process controlling NO_3^-. It is assumed that the flux of NO_3^- into the sediments is balanced by a flux of N_2, the dominant end product

TABLE 8

Nutrient Flux Stoichiometry

Model	Carbon	Nitrogen	Phosphorous	Silica	N:P
Molecular Diffusion (Lower Zone)	100	16.7	1.0	13	16.7
Molecular Diffusion (Interface)	100	24	1.3	23	18.5
Model I	100	22	2.4	50	9.1
Model 2	100	22	1.9	53	11.6
Model 3	100	32	1.0	51	32
Chambers	100	6.5	0.8	23	8
Marine Plankton	100	15.1	0.94	-	16

of denitrification, out of the sediments.

In the lower undisturbed zone of the sediments, molecular diffusive fluxes averaged for 10 San Francisco Bay stations gave a ratio of 100 : 19.5 : 1.2 : - and a N:P ratio of 16.4. Molecular diffusion across the sediment-water interface proceeds at a ratio of 100 : 24 : 1.3 : 23 with a N:P of 18.5. Models 1 and 2 gave similar ratios, 100 : 22 : 2.4 : 50 and 100 : 22 : 1.9 : 53 respectively, with N:P values of 9 and 11. Average values for Model 3 produces the ratio 100 : 32 : 1 : 51 with a N:P value of 33. Flux chambers give the ratio 100 : 6.5 : 0.8 : 23.

For all techniques and models, the NH_4^+ and PO_4^{-3} flux from the sediments appear to be 60 to 70 percent higher than predicted by marine plankton ratios with respect to the carbon flux. This suggests that nitrogen and phosphorus are preferentially stripped from organics during early diagenesis in the sediments.

Nutrient Budget Construction for San Francisco Bay

Rough budgets for carbon, nitrogen, and silica have been constructed for San Francisco Bay in an attempt to assess the relative importance of nutrient regeneration within the sediments. Much of the river, waste water, and productivity data are from Peterson (1978).

Carbon: An average budget for carbon in the San Francisco Bay system is diagrammed in Figure 21. The average flux of T-CO_2 from the sediment to the water column is about 8 to 10 units (mMol/m^2/day). This carbon originates as organic debris which settles out of the overlying water. Using the estimated average sediment accumulation rate of 10 g/m^2/day (Conomos and Peterson, 1977), which corresponds to about 2 mm/yr, and using the percent organic carbon in the sediments, the flux of organic carbon to the sediments can be calculated. Particulate matter in the water column has an average organic carbon content of 2 to 5 percent (from USGS data, L. Schemel, personal communication). Assuming this reflects the nature of the sediments as they arrive at the bottom (3 percent as an average), and using 0.5 percent as a "final" value for sediment organic carbon (Folger, 1972), the flux of carbon to the sediment is about 12 units, 10 of which returns to the water column as dissolved species. The net gain by the sediments is about 2 units.

Peterson (1978) has measured the uptake of CO_2 during primary productivity in the water column. Rates of carbon assimilation range from 35 to 85 units for mid-estuarine waters for net productivity. Dark bottle experiments showed respiration rates of about 20 units. The average gross rate of production is about 60 units, or 6 times as

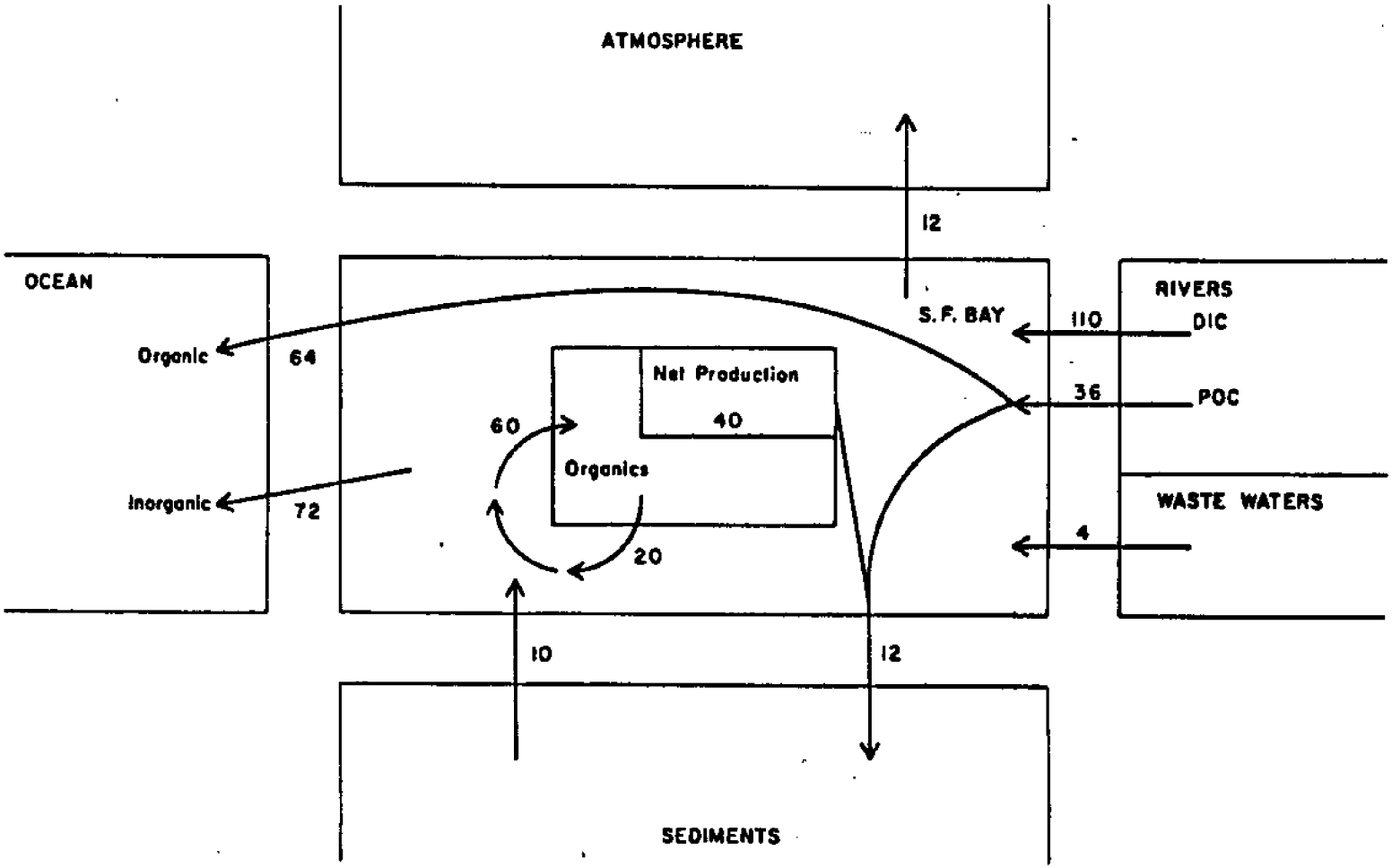

Figure 21. Carbon Budget for San Francisco Bay. Units are mMol/m^2/day.

great as the daily flux from the sediments. Carbon cycling in the water column is twice as important as in the sediments; however, these relationships may change with the seasons, as populations grow and die.

If the rate of carbon carried down to the sediments as organic material is only 12 units, about 64 units must be lost to the ocean waters as organic carbon or transfered out of the system by macro-fauna.

The primary sources for the system include 110 units from the rivers and 4 units from waste waters (Peterson, 1978). Accounting for loss to the atmosphere, ranging from 6 to 20 units and averaging 12 units (Peterson, 1978), the loss of inorganic carbon to the ocean must be about 72 units.

Nitrogen: A nitrogen budget is diagrammed in Figure 22. The average flux of ammonia to the water column determined from the models is about 2 units. This represents nearly 95 to 100 percent of the nitrogen fluxing to the sediments as particulate organics, assuming organics flux to the sediments in the stoichiometric ratio 106:16:1 for C:N:P. River input to the system is about 3 units, primarily particulate organic nitrogen, and waste waters add an additional 2.5 units (Peterson, 1978). The loss to the atmosphere is not known, and consequently, the loss to the

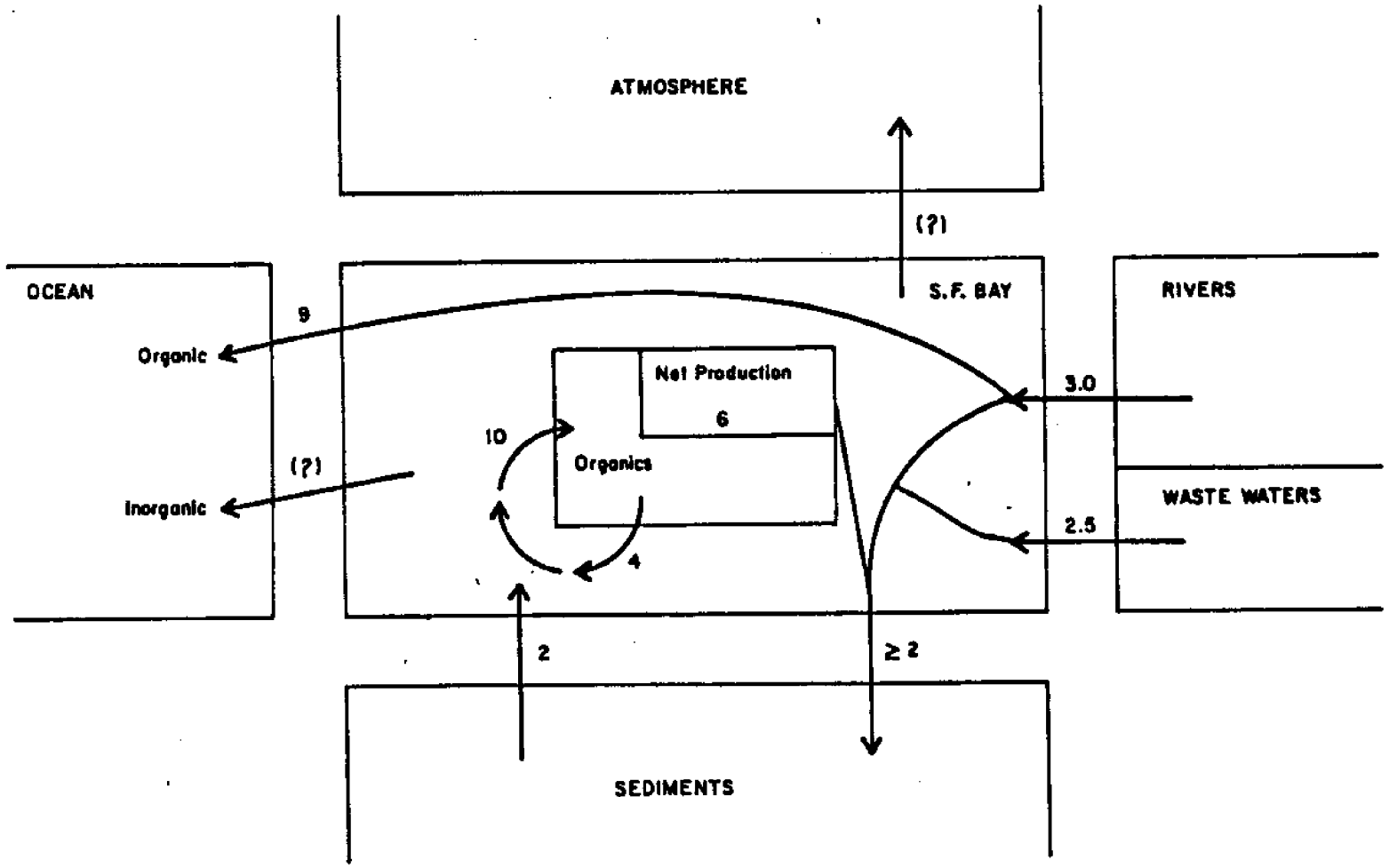

Figure 22. Nitrogen Budget for San Francisco Bay. Units are mMol/m^2/day.

ocean has not been determined. The rate of nitrogen incorporation in net productivity is about 6 units (Peterson, 1978) resulting in a loss of about 4 units as particulate organic nitrogen to the ocean. A value for gross productivity incorporation of nitrogen is not available, but has been estimated on the basis of the stoichiometric relationship to the gross productivity incorporation of carbon, assuming the ratio 106:16:1.

The amount of nitrogen entering the system as fertilizer through run-off is poorly documented, but estimates are as high as 80 to 100 units during high flow periods. This is balanced by a large loss to the ocean, resulting in a near surface plume of NH_4^+ enriched waters extending outside the Golden Gate (Peterson, 1978). Input from the sediment for NH_4^+ -nitrogen is roughly equal to the inputs of river water and waste waters during average flows. Regeneration of NH_4^+ in the sediments is about 1/2 the rate of cycling in the water column, about 1/3 the rate of net productivity incorporation, and 1/5 the rate of incorporation by gross productivity.

Silica: Despite its relatively simple spatial and temporal distribution throughout the system (Peterson et al, 1975), this nutrient is perhaps the most difficult to budget, because of a lack of data. As Figure 23 shows, only a

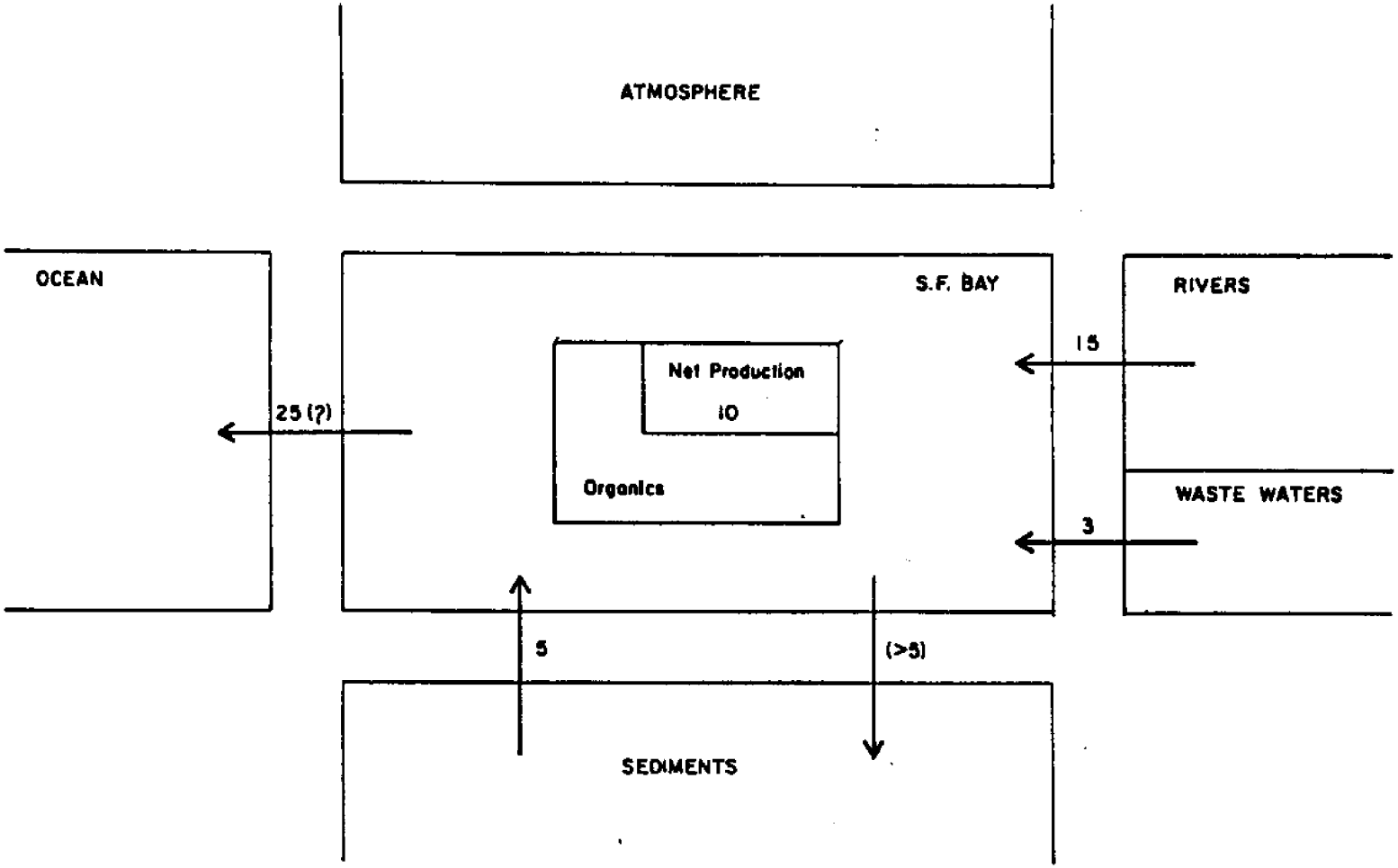

Figure 23. SiO_2 budget for San Francisco Bay. Units are $mMol/m^2/day$.

70

few of the fluxes have been evaluated.

Flux from the sediments, averaging 5 units, is 1/3 the average rate of river input, 15 units (Peterson, 1978), and almost double the rate of waste water input, 3 units (Peterson et al, 1975). The loss to net productivity is 10 units (Peterson, 1978), or roughly twice the flux from the sediments. The loss to gross productivity, to the sediments, and to the ocean are unknown.

CONCLUSIONS

1. Analysis of nutrient concentrations for interstitial waters that have been centrifuged or squeezed from sediments give similar results. Pore water peepers gave equal or lower values, due to incomplete equilibration. Deviations larger than the analytical precision are noted for adjacent cores, but no consistent patterns were found. Parallel core experiments using only centrifugation for extraction show considerable lateral heterogeneity within the sediment and may explain the deviations detected in the techniques comparison. The possible presence of spatial variation over a small area complicates the assessment of temporal variations.

2. Macro-biological activity within sediments facilitates nutrient transport across the sediment-water interface. The mechanism may be modeled as eddy diffusion, direct advection, or increased sediment surface exposed to the water column over which molecular diffusion can occur. These effects produce nutrient fluxes an order of magnitude higher than molecular diffusive fluxes through the undisturbed sediments which underlie the zone of macrobenthic activity. The values of chemical species flux from the sediments to the water column for the three models all fall within a relatively narrow range. Any one or all three transport mechanisms may be operative within the sedimentary environment. Because of the similarity in results, approximate flux values can be calculated using any one of the models without a detailed understanding of the actual mechanism. The average model flux across the sediment-water interface in San Francisco Bay are 10 ± 6.7, 2.3 ± 3, and 5 ± 3.6 mMol/m^2/day for T-CO_2, NH_4^+, and SiO_2, respectively.

3. Using the above flux values calculated from the models, the rate of nutrient regeneration in San Francisco Bay sediments is about 1/2 that of the water column

for carbon and nitrogen. The resulting carbon flux from the sediments is about 1/6 the value of gross carbon assimilation rates for primary productivity in the water column, and 1/4 the net assimilation rate. The NH_4^+-N and SiO_2 flux from the sediment to the water column is about 1/4 the total source of nitrogen and 1/5 the source of dissolved silica to the water column during average river flow conditions.

REFERENCES

Aller, R. C., and Yingst, J. Y., 1978, Biogeochemistry of tube-dwellings: A study of the sedentary polychaete Amphitrite Ornata (Leidy): Jour. Marine Research, 36, 201-254.

Bain, R. C., Jr., and McCarty, J. C., 1965, Nutrient productivity studies in San Francisco Bay, U.S. Public Health Service, Central Pacific Basins Water Pollution Control Proj. Tech. Rept., 116 pp.

Berner, R. A., 1964, An idealized model of dissolved sulfate distribution in recent sediments, Geochim. et Cosmochim. Acta 28, 1497-1503.

Berner, R. A., 1971, Principles of Chemical Sedimentology, McGraw-Hill, New York, 240 pp.

Berner, R. A., 1974, Kinetic models for the early diagenesis of nitrogen, sulfur, phosphorous, and silicon in anoxic marine sediments, in Goldberg, E. D., ed., The Sea, Vol. 5.

Berner, R. A., 1975, Diagenetic models of dissolved species in the interstitial waters of compacting sediments, Am. Jour. of Science 275, 88-96.

Berner, R. A., 1977, Stoichiometric models for nutrient regeneration in anoxic sediments, Limnol. Oceanogr. 22, 781-786.

Bray, J. T., Bricker, O. P., and Troup, B. N., 1973, Phosphate in interstitial waters of anoxic sediments: Oxidation effects during sampling procedures, Science 482, 1362-1364.

Conomos, T. J., and Peterson, D. H., 1977, Suspended-particle transport and circulation in San Francisco Bay: an overview, in Cronin, ed., Estuarine Processes, Vol. 2, Academic Press, New York, 82-97.

Dales, R. P., 1961, Oxygen uptake and irrigation of the burrow by three terebellid polychaetes, Physiol. Zool. 34, 306-311.

Fanning, K. A., and Pilson, M. E., 1971, Interstitial silica and pH in marine sediments: some effects of sampling procedures, Science 373, 1228-1231.

Filice, F. P., 1958, Invertebrates from the estuarine portions of San Francisco Bay and some factors influencing their distribution, The Wasmann Jour. of Biol. 16, 159-216.

Folger, D. W., 1972, Texture and organic carbon content of bottom sediments in some estuaries of the United States, in Nelson, B. W., ed., Environmental framework of coastal plain estuaries, Geol. Soc. Am. Memoir 133, 391-408.

Goldhaber, M. B., Aller, R. C., Cochran, J. K., Rosenfeld, J. K., Martens, C. S., and Berner, R. A., 1977, Sulfate reduction, diffusion, and bioturbation in Long Island Sound sediments: Report of the FOAM Group, Am. Jour. of Science 277, 193-237.

Grundmanis, V. and Murray, J. W., 1977, Nitrification and denitrification in marine sediments from Puget Sound, Limnol. Oceanogr. 22, 804-813.

Hale, S., 1974, The role of benthic communities in the nutrient cycles of Narragansett Bay, M.S. Thesis, University of Rhode Island, 129 pp.

Hammond, D. E., 1975, Dissolved gases and kinetic processes in the Hudson River Estuary, Ph.D. dissertation, Columbia University, 161 pp.

Hammond, D. E., 1977, The uptake of oxygen by Los Angeles Harbor and San Francisco Bay sediments, in The planning and management of California's coastal resources, 1976-1977, U.S.C. Sea Grant Inst. Prog. Annual Report, 28-32.

Hammond, D. E., and Fuller, C., 1978, The use of Radon-222 as a tracer in San Francisco Bay, in Conomos, T. J. ed., Symp. on San Francisco Bay, Am. Assoc. Adv. Sci., in press.

Hesslein, R. H., 1976, The fluxes of CH_4, T-CO_2, and NH_3-N from sediments and their consequent distribution in a small lake, Ph.D. Dissertation, Columbia University, 186 pp.

Hines, W. G., 1973, A review of wastewater problems and wastewater management planning in the San Francisco Bay Region, California, USGS Open-File Report, Menlo Park, Calif., 45 pp.

Hobbie, J. E., Copeland, B. J., and Harrison, W. G., 1975, Sources and fates of nutrients of the Pamlico River Estuary, N. Carolina, in Cronin, L. E., Estuarine Research, Vol. 1, New York Academic Press, 287-302.

Jaworski, N. A., Lear, E. W., Jr., and Villa, O., 1972, Nutrient management in the Potomac Estuary, in Likens, G. E., ed., Nutrients and Eutrophication, Special Symposia Vol. 1, Am. Soc. of Limnol. and Oceanography, 246-273.

Jorgensen, B. B., 1977a, Bacterial sulfate reduction within reduced microniches of oxidized marine sediments, Mar. Biol. 41, 7-17.

Jorgensen, B. B., 1977b, The sulfate cycle of a coastal marine sediment (Limfjorden, Denmark), Limnol. Oceanogr. 22, 814-832.

Li, Y. H. and Gregory, S., 1974, Diffusion of ions in sea water and in deep-sea sediments, Geochim. et Cosmochim. Acta 38, 703-714.

Matisoff, G., Bricker, O. P., III, Holdren, G. R., Jr., and Kaerk, P., 1975, Spatial and temporal variations in the interstitial water chemistry of Chesapeake Bay Sediments, in Church, T. M., ed., Marine Chemistry in the Coastal Environment, Am. Chem. Soc., Symposium Series 18, 343-363.

McCaffrey, R. J., Meyer, A. C., and Bender, M., 1978, Benthic fluxes of nutrients and manganese in Narragansett Bay, Rhode Island, submitted to Limnology and Oceanography.

McCarthy, J. J., Taylor, W. R., and Taft, J. T., 1975, The dynamics of nitrogen and phosphorous cycling in the open waters of Chesapeake Bay, in Church, T. M., ed., Marine Chemistry in the Coastal Environment, Am. Chem. Soc., Symposium Series 18, 664-681.

McCulloch, D. S., Peterson, D. H., Calson, P. R., and Conomos, T. J., 1970, Some effects of fresh water inflow on the flushing of South Bay San Francisco Bay: A preliminary report, USGS Circular 637, 27 pp.

Miller, L., 1977, Effects of cold storage on nutrient concentrations for ammonia, phosphate, silicate, and nitrate; Unpublished Report, University of Southern California.

Mullin, J. B., and Riley, J. P., 1955, Colorimetric determination of silicate with special reference to sea and natural waters. Anal. Chim. Acta 12, p. 162-176.

Murphy, J., and Riley, J. P., 1962, A modified single solution for the determination of phosphate in natural waters, Anal. Chim. Acta 27, p. 31-36.

Nichols, F. H., 1973, A review of benthic faunal surveys in San Francisco Bay, USGS Circular 677, 20 pp.

Nixon, W. S., Oviatt, C. A., and Hale, S. S., 1976, Nitrogen regeneration and the metabolism of coastal marine bottom communities, in Anderson, J. M., and Macfayden, A., eds., The Role of Terrestrial and Aquatic Organisms in Decomposition Processes, Blackwell Scientific Pub., Oxford, 269-283.

Pestrong, R., 1970, Tidal flat sedimentation at Cooley Landing, S. W. San Francisco Bay, Office of Naval Research Technical Report, Contract Nonr-4430(00), 53 pp.

Peterson, D. H., 1978, Sources and Sinks of biologically reactive substances (oxygen, carbon, nitrogen, and silica) North San Francisco Bay, in Conomos, T. J. ed., Symposium on San Francisco Bay, Am. Assoc. Adv. Sci., in press.

Peterson, D. H., Conomos, T. J., Broenkow, W. W., and Scrivani, E. P., 1975, Processes controlling the dissolved silica distribution in San Francisco Bay, in Cronin, L. E., ed., Estuarine Research Vol. 1, New York Academic Press, 153-187.

Presley, B. J., 1971, Determination of selected minor and major inorganic constituents, in Initial Reports of the Deep Sea Drilling Project, Vol. 7, U.S. Government Printing Office, 1749-1752.

Redfield, A. C., Ketchum, B. H., and Richards, F. A., 1963, The influence of organisms on the composition of sea water, in Hill, M. N., ed., The Sea, Vol. 2, Wiley, 26-77.

Reeburgh, W. S., 1967, An improved interstitial water sampler, Limnol. Oceanogr. 12, 163-165.

Rittenberg, S. C., Emery, K. O., and Orr, W. L., 1955, Regeneration of nutrients in sediments of marine basins, Deep Sea Research 3, 23-45.

Sholkovitz, E., 1973, Interstitial water chemistry of the Santa Barbara Basin sediments, Geochim. et Cosmochim. Acta 37, 2043-2073.

Simpson, H. J., Hammond, D. E., Deck, B. L., and Williams, S. C., 1975, Nutrient budgets in the Hudson River Estuary, in Church, T. M., ed., Marine Chemistry in the Coastal Environment, Am. Chem. Soc. Symposium Series 18, 618-635.

Solorozanc, L., 1969, Determination of ammonia in natural waters by the phenol hypochlorite method, Limnol. Oceanogr. 14, 799-801.

Storrs, P. M., Selleck, R. E., and Pearson, E. A., 1963, A comprehensive study of San Francisco Bay 1961-1962: second annual report, Univ. California San. Eng. Res. Lab., Rept. No. 63-4, 323 pp.

Storrs, P. M., Selleck, R. E., and Pearson, E. A., 1964, A comprehensive study of San Francisco Bay 1962-1963: third annual report, Univ. California San. Eng. Res. Lab., Rept. No. 64-3, 227 pp.

Strickland, J. D. H., and Parsons, T. R., 1972, A Practical Handbook of Sea water analysis, Fisheries Research Board of Canada, Bulletin 167, 310 pp.

Vanderborght, J. P., Wollast, R., and Billen, G., 1977a, Kinetic models of diagenesis in disturbed sediments Part 1: Mass transfer properties and silicate diagenesis, Limnol. Oceanogr. 22, 787-793.

Vanderborght, J. P., Wollast, R., and Billen, G., 1977b, Kinetic models of diagenesis in disturbed sediments Part 2: Nitrogen diagenesis, Limnol. Oceanogr. 22, 794-803.

Whelan, T., 1974, Methane, CO_2, and $SO_4^=$ from interstitial waters of coastal marsh sediments, in Estuarine and Coastal Marine Science Vol. 2, 407-415.

APPENDIX A

San Francisco Bay Station Locations

Station	Water Depth* (m)	Latitude	Longitude
Sta 13	10.5	38° 01' 50"N	122° 21' 55"W
Sta 13.22	4	38° 03' 00"	122° 21' 21"
Sta 14	11.5	38° 00' 27"	122° 24' 15"
Sta 14C	3	38° 02' 15"	122° 25' 00"
Sta RB 2	0.5	37° 52' 15"	122° 29' 00"
Sta 18	15	37° 51' 00"	122° 23' 47"
Sta 18.20 & 18B	4.5	37° 51' 15"	122° 22' 30"
Sta 20.46	11.5	37° 49' 17"	122° 20' 00"
Sta 27	11	37° 37' 05"	122° 17' 40"
Sta 28	14.5	37° 36' 05"	122° 16' 10"
Sta 28C	0.5	37° 35' 55"	122° 20' 47"
Sta 28E	3	37° 36' 20"	122° 17' 34"
Sta 29.3E	2	37° 35' 23"	122° 12' 50"

*Depth at Mean Lower Low Water

APPENDIX B

Core Logs

Sta 28C 3/77, 23 cm. deep, worm tubes with active polychaetes down to about 12 cm., very shelly, grey clay with shells, H_2S smell throughout.

Sta 27 3/77, Shelly top, turning darker at 9-12 cm., silty clay. Strong H_2S odor and very dark greyish black color below 25 cm.

Sta 13 3/77, Brown silty sand at top with shell fragments extending down to 6 cm. Dark grey black below 6 cm. H_2S detected below 10-13 cm. A lense of brown sand between 45 and 60 cm. depth.

Sta 14C 3/77, Live polychaetes observed down to 32 cm. Brown silty sand at top, changing to shelly layer at 5 cm. and silty clay below.

Sta 18B 3/77, Small red worms detected down to 30 cm., concentrated at 6 to 10 cm. and at 16 to 20 cm; Fine-grained high permeable silty clay down to 30 cm., with a lense of orange sand at 26 cm. and highly compacted, low permeable silty clay below 38 cm.

Sta 28C 7/77, Brown silt down to 1 cm. with grey silty clay below and a brown sand zone at 6 to 8 cm. Shell fragments throughout. Black clay clumps observed at 4 cm.

Sta 27 7/77, Large shell fragments throughout. Highly compacted below 8 cm., with low porosity.

Sta 13 7/77, Brown silty sand at top 2 cm. with dark grey silty clay below. Brown silt layer at 22 cm. Some tubes noted for top two intervals.

Sta 28C 10/77, Silt and clay in shell fragments down to 10 cm. with dark grey clay below.

APPENDIX B (Cont.)

Core Logs

Sta 28E 10/77, Coarse shell fragments with silt and sand down to the bottom of core, 20 cm.

Sta 28 10/77, Silt down to 40 cm., with silty clay below. Live red worms detected down to 28 cm. Burrows concentrated around 10-13 cm. interval.

APPENDIX C

The Sulfate Problem

Several of the measured values for near surface pore water SO_4^{-2} exceeded water column concentrations. This suggested a possible problem with the technique. Sulfate was redetermined on those pore water samples which had originally shown high apparent concentrations. The results are listed in Table C-1. Some sample values remained high, such as for Station 28C 3/77 0-3 cm while pore water sulfates for other intervals decreased. Chlorinity determinations have shown that the sample which gave high results for the second determinations has undergone evaporation during the storage period of 2 to 8 months. This evaporation may have occurred before the initial measurement. Sulfate/chlorinity ratios for these samples are equal or less than the sea water ratio.

Samples which showed initially high sulfate concentration but lower values for the redetermined concentration, such as Station 28C 7/77 2-4 cm, showed no appreciable evaporation, based on chlorinity. It is possible that dissolved organics are present within the pore waters which precipitate out during the addition of the acidic $BaCl_2$ spike. Goldhaber et al (1977) noted that the pore

water from Long Island Sound became cloudy upon acidification during gravimetric determination of SO_4^{-2} and attributed this to dissolved organics. They avoid the problem by filtering acidified samples before precipitation.

The presence of these precipitated organics may have caused an absorption of excess barium on the filter during the initial measurements. The lower sulfate values obtained in the second measurement suggest that the organics break down during storage and present no interference. Table C-2 shows the results of a series of experiments designed to determine the positive interference of organics. For the two sample waters used, the second determination reproduced the high values for Sta 28C 3/77 0-3, while a decrease of about 4 mM (-13 percent) was determined for Station 28 10/77 20-24 cm. Pore waters from these stations were (1) acidified with a few drops of 8N HCl before precipitation, (2) treated with H_2O_2 added to the sample before precipitation, and (3) rinsed after precipitation with a NaOH solution. The measured concentrations showed very little change in the course of these experiments (within the analytical error) and suggest no organics were interferring with the SO_4^{-2} determination at the time of the test. High values at Station 28C 3/77 0-3 cm were shown to be due to evaporation.

South Bay stations seemed to be most affected by the high apparent concentrations, usually in the second and third intervals within the sediments (6 to 10 cm). Re-determinations of "aged" samples showed the interference had increased apparent concentrations by 4 to 14 percent in the upper sediment zone with no appreciable increase for the sediments below the mixed zone. Sulfate data listed in figures and tables have been corrected for organic interference and evaporation effects. Samples which were not directly measured a second time were corrected by using a factor determined by adjusting the $SO_4^{=}/Cl^{-}$ ratio to the water column Cl^{-} concentrations, or by subtracting an average factor which was determined from the percent change listed in Table C-1.

TABLE C-1

Sulfate and Chlorinity Determinations

Station and Interval	First $SO_4^=$ Measurement (mM)	Second $SO_4^=$ Measurement (mM)	Cl^-(**) (meq/l)	$SO_4^=/Cl^-$(*) (%)
Standard Sea Water	27.5	27.5	532	5.16
S.F. Bay (South)	26	26	517	5.05
Sta 13 3/77				
36-40 cm	14.9	13.8	396	3.49
44-48 cm	12.8	13.1	495	2.65
60-64 cm	10.0	9.3	383	2.42
Sta 14C 3/77				
6-9 cm	29.8	26.5	-	-
Sta 27 3/77				
35-39 cm	11.2	10.5	470	2.23
42-46 cm	8.9	9.6	536	1.7
64-68 cm	3.7	3.0	431	0.71
Sta 27 3/77				
2-5 cm	30.4	28	542	5.17
8-13 cm	21.8	21.8	475	4.59
Sta 28 10/77				
10-13 cm	30.2	28.7	510	5.62
20-24 cm	31.1	27.9	491	5.51
Sta 28C 3/77				
0-3 cm	31	33.5	742	4.52
18-23 cm	20.6	20.1	-	-
Sta 28C 7/77				
2-4 cm	31.8	26	538	4.83
10-14 cm	23.8	24.5	483	5.07

* The ratio is expressed as a molar percentage, calculated from the second $SO_4^=$ measurement.

** Measured at the time of the second sulfate analysis.

TABLE C-2

Organic Interference Tests for $SO_4^=$ Method*

Sample	$(SO_4^=)^{(1)}$ (mM)	$(SO_4^=)^{(2)}$ (mM)	Acid (mM)	H_2O_2 (mM)	Base Wash (mM)
Standard Water 1	27.5	27.5	27	-	-
Standard Water 2	27.5	27.5	27.5	25.8	26
Standard Water 3	27.5	27.5	26.3	-	-
Sta 28C 3/77 0-3 cm	31	32	28.8	31	31.8
Sta 28 10/77 20-24 cm	31.1	27.1	28.3	28.6	-

*Tests are described in Appendix C

(1)Initial measurement of $SO_4^=$

(2)Second measurement of $SO_4^=$ (Redetermination)

APPENDIX D

Peeper Equilibration

The pore water peeper used at San Francisco Bay 10/77 was removed from the sediments after 8 days. Chlorides were determined for most of the intervals and are listed in the table below. The Cl^- concentration in the waters at Station 28C, the peeper site, was approximately 517 mM, calculated from salinity measurements.

Depth Interval	Cl^- (mM)	% Equilibrated (using 517 mM)
3	539	104
4	540	104
5	539	104
10	491	95
13	460	89
15	464	90
18	468	91
21	459	89
22	451	87
26	433	84
27	438	85

While the top intervals appear to be fully equilibrated, there is a decrease with depth. This may represent a dilution of Cl^- in the interstitial waters by fresh water intrusion, or may be an actual equilibration problem due to differential mass transfer coefficients in the lower sediments. Lower sediments are more compacted, with lower permeability and cooler temperatures. This would tend to lower the coefficient of molecular diffusion for the sediments, (D_s), and increase the time

constants for mass transfer.

APPENDIX E

Notations and Abbreviations

C_{IW}	Pore water concentration in upper mixed zone of sediments
C_{WC}	Water column concentration
D_t	Temperature dependent Coefficient of Molecular Diffusion
D_s	Coefficient of Diffusion for a species in sediments
D_{M1}	Turbulent Diffusivity Coefficient for Model 1
dc/dx	Concentration gradient with depth
dc/dx_L	Concentration gradient through the lower undisturbed zone
dc/dx_U	Concentration gradient in the mixed zone
dc/dx_I	Concentration gradient across the sediment-water interface
dc/dx_3	Average concentration gradient between Polychaete burrows
f_w	Ratio of tube surface area to sediment surface area
h	Depth to which Rn-222 deficiencies can be detected
J_{MD}	Molecular diffusive flux
J_{MDL}	Molecular diffusive flux through the lower sediment zone
J_{MDI}	Molecular diffusive flux across the sediment-water interface

J_U	Flux through the upper sediment zone
J_{M1}	Model 1 flux
J_{M2}	Model 2 flux from pumping
J_{RnP}	Flux of Rn-222
J_{MDRn}	Molecular diffusive flux of Rn-222
J_{M3}	Model 3 flux
R	Average areal pumping rate of Polychaetes (cm/sec)
P	Production rate of Rn from Ra per unit volume
S_U	Concentration of Rn-222 in the upper zone
S_{eq}	Equilibrium concentration of Rn-222 in the sediments
units	Millimoles/meter^2 -day mM/m^2 day
λ	Decay constant
$\emptyset$	Porosity
θ	Tortuosity
x_b	Average distance between burrows in the sediments
r_b	Average burrow radius
p	Density of burrows in the sediments
b_s	Number of tubes extending to the surface of the radiograph

l_b	Length of an individual worm burrow
d_b	Maximum depth to which burrows extend
A_r	Area of sediment surface represented by radiograph